NATIONAL AERONAUTICS AND SPACE ADMINISTRATION

TECHNICAL REPORT
R-156

RADIANT HEAT TRANSFER TO ABSORBING GASES ENCLOSED IN A CIRCULAR PIPE WITH CONDUCTION, GAS FLOW, AND INTERNAL HEAT GENERATION

By THOMAS H. EINSTEIN

1963

For sale by the Superintendent of Documents, U.S. Government Printing Office,
Washington, D.C., 20402. Price 35 cents

TECHNICAL REPORT R-156

RADIANT HEAT TRANSFER TO ABSORBING GASES ENCLOSED IN A CIRCULAR PIPE WITH CONDUCTION, GAS FLOW, AND INTERNAL HEAT GENERATION

By THOMAS H. EINSTEIN

Lewis Research Center
Cleveland, Ohio

CONTENTS

TECHNICAL REPORT R-156

RADIANT HEAT TRANSFER TO ABSORBING GASES ENCLOSED IN A CIRCULAR PIPE WITH CONDUCTION, GAS FLOW, AND INTERNAL HEAT GENERATION

By Thomas H. Einstein

SUMMARY

A two-dimensional analysis is presented for determining the heat transfer to a gray uniformly absorbing gas enclosed in a black circular pipe under the combined influence of radiation, gas flow through the pipe, and thermal conduction in the gas. The analysis also takes into account the presence of distributed energy sources in the gas.

Specific results are obtained for a pipe with a length to diameter ratio of 5 and for a range of gas opacity from 1.0 to 10.0. The ends of the pipe consist of porous black plugs that simulate the radiation environment external to the pipe but permit flow through the pipe. All the results are presented in dimensionless parameters for generality.

It was found that when an absorbing gas flowing through a pipe is heated only by radiation emitted from isothermal walls of the pipe, the heat transmitted to the gas goes through a maximum as the opacity of the gas is increased.

Results are also presented for heat transfer to a flowing gas and the pipe walls by radiation emitted from a heat-generating gaseous core in the center of the pipe. For these specific results, the radius of the heat-generating cylindrical gaseous core is 0.2 of the pipe radius. It is shown that the percentage of heat generated that is radiated to the wall can be made negligibly small if both the gas opacity and the gas flow rate in the annulus surrounding the core are made sufficiently high.

Finally, results are presented for one-dimensional radial radiant heat transfer from a heat-generating gaseous core through a stationary absorbing gas to the walls of the pipe. These results are compared with a solution for the emissive power distribution in the gas obtained by using the Rosseland diffusion approximation with a jump boundary condition, and good agreement between the two methods is obtained.

INTRODUCTION

Recently, there has been a significant increase of interest in heat-transfer problems associated with thermal-radiation-absorbing gases. Nearly all gases, when in the dissociated or ionized state, absorb radiation to some extent. Many gases, such as water vapor and carbon dioxide, are even fair absorbers in their normal molecular states at moderate temperatures. Even gases that do not absorb radiation can be made into effective absorbers if they are seeded with microscopic dust particles or powders such as carbon black. The recent surge of interest in this area is related to the current importance of high-temperature problems associated with space-vehicle reentry, heat transfer from electric arcs and other high-temperature plasmas, and energy transport in in gaseous nuclear reactors.

Reference 1 deals with the interaction between radiation and thermal conduction and with radiant heat transfer from constant-temperature surfaces to flowing radiation-absorbing gases. Two-dimensional results were obtained for the case of a finite length channel formed between two semi-infinite parallel flat plates. That geometry was chosen in order to simplify the analysis and presentation of results in that report as much as possible. Although many interesting and important generalized results were obtained with regard to the effects of flow on radiant transfer to an absorbing gas and the interaction between radiation and conduction, the semi-infinite parallel-plate geometry of that report made interest

in the specific results obtained therein somewhat academic.

It is the purpose of this report to apply the method of analysis used in reference 1 to a geometry of more practical interest, a circular pipe of finite length, and to present results for radiant heat transfer to absorbing gases enclosed in such a pipe. Typical problems to which this analysis might be applied are radiant heating of an absorbing gas flowing through a heated pipe, the heating of the walls of a pipe by an enclosed plasma jet or electric arc, or heat transfer in a coaxial-flow gaseous reactor.

Previous work in the analysis of radiant heat transfer to absorbing gases in a cylindrical pipe is described in references 2 and 3. The analysis of reference 2 is for a gray gas of uniform absorptivity flowing in a black cylindrical pipe. Some of the assumptions used in the analysis, however, render the results valid only when reemission of radiation by the gas may be neglected. Reference 3 applies the method of analysis of reference 4 to the heating of an absorbing medium in a cylindrical pipe and treats the case of a nongray gas enclosed in a pipe that has a partly reflecting (gray) surface. The analysis, however, does not allow for radial temperature gradients in the medium. Also, although the method of analysis is presented, no results are given.

The two-dimensional analysis for a cylindrical pipe presented in this report follows along the same lines as that given in reference 1. For the sake of simplicity, the present analysis assumes that conditions in the pipe are axisymmetric, and it is limited to a gray gas of uniform absorptivity enclosed in a cylinder whose interior surfaces are black. The analysis, however, could be extended to cover nongray gases by applying the method of reference 4, in which a nongray gas is approximated by a mixture of gray gases.

Results are presented herein for (1) heating a flowing gas by radiation from a constant temperature pipe wall, and (2) for heating the gas and the interior surface of the pipe by radiation from energy sources distributed uniformly in a cylindrical inner concentric core of the gas, the diameter of which is 0.2 that of the pipe. All results are presented in terms of dimensionless parameters to obtain maximum generality.

ANALYSIS

A two-dimensional analysis of radiant heat transfer is presented for a gray gas of uniform absorptivity enclosed in a cylindrical pipe of finite length as shown in figure 1. The interior surface of the pipe is black, and conditions at the

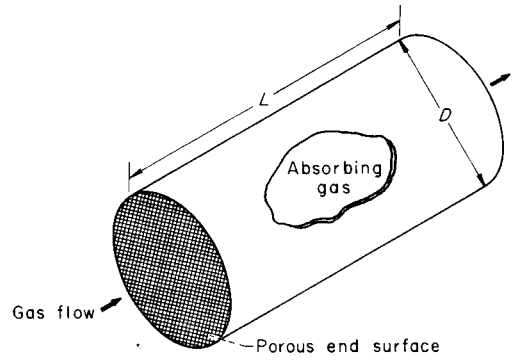

FIGURE 1.—Cylindrical pipe containing radiation-absorbing gas.

ends of the pipe are represented by porous black surfaces. These pseudo end surfaces are assumed to be black in order to simulate the radiant properties of the environment exterior to the pipe in calculating the radiant interchange between this environment and the gas and surfaces in the interior of the pipe; they are assumed porous to allow for the flow of gas through the ends of the pipe. The analysis takes into account not only the radiant interchange in the pipe but also the simultaneous effects of gas flow and thermal conduction.

For the purpose of simplicity, however, as is often done in convection heat-transfer problems, the axial component of conduction is neglected, which leaves only the radial component to be considered. Allowance is also made for distributed energy sources in the gas. The conditions in the pipe are also assumed to be axisymmetric. A rigorous treatment of this problem requires the solution of the following two-dimensional integro-differential equation, which represents the heat balance on an infinitesimal volume of gas dV.

located at position $\vec{r}_o$ in the interior of the pipe:

$$4k\sigma T^4(\vec{r}_o)+Gc_p\left.\frac{\partial T(\vec{r})}{\partial x}\right|_{\vec{r}=\vec{r}_o}-\frac{\lambda}{\rho}\frac{\partial}{\partial\rho}\left[\rho\frac{\partial T(\vec{r})}{\partial\rho}\right]\Bigg|_{\vec{r}=\vec{r}_o}=k\iiint\sigma T^4(\vec{r})f(\vec{r}-\vec{r}_o)\mathrm{d}v$$
$$+k\iint\sigma T_s^4(\vec{r})g(\vec{r}-\vec{r}_o)\mathrm{d}A+q'''(\vec{r}_o) \quad (1)$$

where

$q'''(\vec{r}_o)$	heat generation in the gas per unit volume at $\vec{r}_o$
$4k\sigma T^4(\vec{r}_o)$	radiant energy emitted per unit volume at $\vec{r}=\vec{r}_o$
$Gc_p\left.\frac{\partial T(\vec{r})}{\partial x}\right\|_{\vec{r}=\vec{r}_o}$	rate of enthalpy increase of the flowing gas at $\vec{r}=\vec{r}_o$
$\frac{\lambda}{\rho}\frac{\partial}{\partial\rho}\left[\rho\frac{\partial T(\vec{r})}{\partial\rho}\right]\Big\|_{\vec{r}=\vec{r}_o}$	net conduction heat transfer per unit volume at $\vec{r}=\vec{r}_o$
$k\iiint\sigma T^4(\vec{r})f(\vec{r}-\vec{r}_o)\mathrm{d}v$	radiation absorbed per unit volume at $\vec{r}_o$ from emission given off by the rest of the gas in the cylinder
$k\iint\sigma T_s^4(\vec{r})g(\vec{r}-\vec{r}_o)\mathrm{d}A$	radiation absorbed per unit volume at $\vec{r}_o$ from emission of pipe wall and end surfaces

(All symbols are defined in appendix A.)

Unfortunately, even in the case where thermal conduction and flow are absent, equation (1) is not easily solved for a cylindrical geometry, though solutions have been obtained for a spherical geometry (ref. 5) and infinite parallel flat plates (ref. 6). Consequently, the only feasible way of obtaining a solution to equation (1) for a cylindrical geometry, even in the absence of conduction or flow, is by resorting to a scheme such as that described in reference 1, in which the interior of the cylinder is divided into a finite number of zones, and the two-dimensional integrodifferential equation is approximated by a system of algebraic equations. Thus, in the present situation, the interior of the cylinder is broken up into 50 gas-ring zones of rectangular cross section, 10 zones axially and 5 zones radially, as shown in figure 2. The cross sections of all these gas zones are identical, and the zones themselves are toroidal rings of rectangular cross section except for the innermost zones, which are solid cylinders whose radii are equal to 0.2 of the radius of the pipe. Figure 2 is a cutaway view of the pipe that shows the division of the interior into the zones, as described previously, and the shape of each zone. The cylindrical and end surfaces of the pipe are similarly divided into surface zones whose boundaries correspond with those of the adjoining gas zones described previously. Thus, the cylindrical surface is divided into ten equal size surface zones of cylindrical shape, of which the length of each is 0.1 that of the whole pipe. Similarly, each of the end surfaces is divided into five radial surface zones of annular shape, the width of which is 0.2 of the pipe radius. Again, the innermost surface zone on the end degenerates into a circle whose radius is 0.2 of the pipe radius.

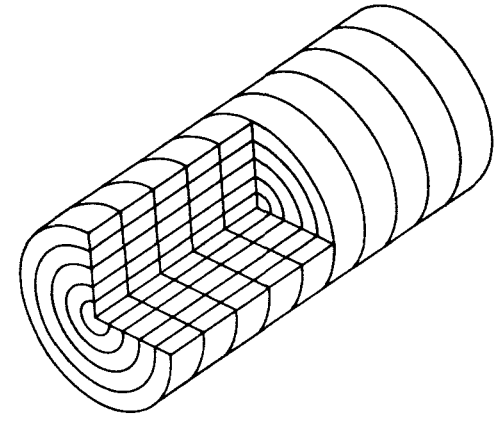

FIGURE 2.—Interior of pipe illustrating division of gas into toroidal zones of rectangular cross section.

APPLICATION OF HEAT-BALANCE EQUATIONS AT ZONE CENTERS

Given the preceding division of the gas in the pipe into 50 zones, the solution to equation (1) may be approximated by writing heat-balance equations on infinitesimal volumes located at the centers of the cross sections of each of the 50 gas zones. The circumferential position in the zones of these infinitesimal volumes is immaterial, since conditions in the pipe are assumed to be axisymmetric. The problem now to be solved is to determine the temperature distribution in the gas and the heat flux to the surfaces for a given surface temperature distribution and for given distribution of energy sources in the gas. The surface temperatures are specified for each of the surface zones on the cylindrical wall and both ends. The temperature of each surface zone is assumed to be uniform over that zone but may vary from one surface zone to the next. Thus, the temperature distribution on a surface is approximated by a stepwise temperature distribution over the zones comprising that surface. The heat-generation rate per unit volume is specified for each of the gas zones (this quantity will in many cases be zero for some or all of the zones). Again, this power density is assumed to be uniform over any given zone so that the total power produced by the sources in that gas zone is obtained by multiplying the power density by the zone volume. Thus, the distribution of energy sources in the gas is approximated by the stepwise variation of power generation over the gas zones.

Again, the problem to be solved is: Given a temperature distribution on the surface boundaries of the pipe and a distribution of internal energy sources in the gas, find the resulting temperature distribution in the gas and the heat transfer between the gas and the surfaces. As mentioned before, an approximation to the solution of the problem is obtained by applying equation (1) to the heat balances on the infinitesimal volume elements at the centers of the cross sections of each of the gas zones. In order to replace the integrodifferential equation with algebraic equations, it becomes necessary to approximate the derivatives in equation (1) with algebraic difference quotients in terms of the gas-zone-center temperatures and the integrals in terms of finite sums that are algebraic functions of the gas-zone-center temperatures. Since there are 50 gas zones, there are 50 separate heat-balance equations and also 50 unknowns, namely, the temperatures at the centers of the cross sections of the gas zones. The algebraic-difference-quotient approximations for the derivatives are obvious. The presentation of the integrals in terms of the unknown gas-zone-center temperatures is more involved and is the subject of the following paragraphs. In any case, since the regions of integration are divided into zones, the integrals over the pipe in equation (1) may be exactly represented by obtaining the integrals for each zone and then summing these zone integrals over all the zones in the pipe.

Each of the 50 zones is labeled by a dual subscript (i, j), where i is the position along the length of the pipe and j represents the radial position from the center of the pipe to the wall. Figure 3 gives the cross section of the pipe along the centerline showing the gas zone cross sections and describing the manner of labeling given previously. Consequently, the heat-balance equation on an infinitesimal volume element at the center of the $(i, j)^{\text{th}}$ zone may be written as follows:

$$
\begin{aligned}
&4k\sigma T_{i,j}^4 + Gc_p \frac{T_{i+1,j} - T_{i-1,j}}{2\Delta x} \\
&- \lambda \left(\frac{T_{i,j+1} + T_{i,j-1} - 2T_{i,j}}{\Delta \rho^2} \right) - \frac{\lambda}{\rho_{i,j}} \left(\frac{T_{i,j+1} - T_{i,j-1}}{2\Delta \rho} \right) \\
&= q'''_{i,j} + k \sum_{m=1}^{10} \sum_{n=1}^{5} \iiint \sigma T^4(\vec{r}_{m,n}) f(\vec{r}_{m,n} - \vec{R}_{i,j}) \mathrm{d}v \\
&+ k \sum_{m=1}^{10} \sigma T_{w_m}^4 \iint g_w(\vec{r}_m - \vec{R}_{i,j}) \mathrm{d}A \\
&+ k \sum_{l=1}^{2} \sum_{n=1}^{5} \sigma T_{e_{l,n}}^4 \iint g_e(\vec{r}_n - \vec{R}_{i,j}) \mathrm{d}A \\
&\qquad \text{for } i = 1\text{-}10;\ j = 1\text{-}5 \qquad (2)
\end{aligned}
$$

Obviously, the form of the derivative approximations, which appear in equation (2), needs to be modified along the surface boundary of the pipe for $i=1$, 10 or $j=5$. Here, $\vec{R}_{i,j}$ represents the position vector at the center of the cross section of the $(i, j)^{\text{th}}$ gas zone, $\vec{r}_{m,n}$ is the position vector of a point in the $(m, n)^{\text{th}}$ gas zone, and $\vec{r}_m$ and $\vec{r}_n$ the position vectors of points on the m^{th} wall-surface zone or n^{th} end-surface zone, respectively. The subscript l in the last summation denotes the two end surfaces of the pipe. As mentioned earlier, the surface temperatures

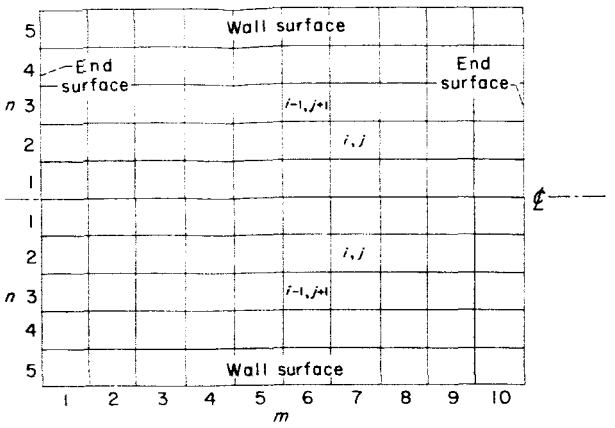

FIGURE 3.—Cross section of circular pipe illustrating division into 50 toroidal ring gas zones, 10 wall-surface zones, and 5 end-surface zones on each end.

on the pipe, which are given, are assumed to be constant over each of the surface zones; therefore, they may be taken outside the integral sign in the integral over each zone, as illustrated in the last two terms of equation (2). The temperatures in the gas zones, however, are not assumed to be uniform over each zone, as will be discussed shortly and, thus, for the time being will remain inside the integral sign. The factor $f(\vec{r}_{m,n}-\vec{R}_{i,j})$ is the exchange factor between a ring of gas of infinitesimal cross section and volume dv through position $\vec{r}_{m,n}$ in the cross section of the $(m, n)^{\text{th}}$ gas zone and the infinitesimal volume located at position $\vec{R}_{i,j}$ at the center of the cross section of the $(i, j)^{\text{th}}$ gas zone, on which the energy balance is being taken. Similarly, the factor $g_w(\vec{r}_m-\vec{R}_{i,j})$ is the exchange factor between a surface ring of infinitesimal width and area dA on the cylindrical wall at position $\vec{r}_m$ on the wall-surface zone and the infinitesimal gas volume at position $\vec{R}_{i,j}$. Finally, $g_e(\vec{r}_n-\vec{R}_{i,j})$ is the exchange factor between an annular surface ring of infinitesimal width and area dA at position $\vec{r}_n$ on the n^{th} end-surface zone and the infinitesimal gas volume at position $\vec{R}_{i,j}$. A thorough derivation and a description of these three exchange factors are given in appendix B.

ALLOWANCE FOR VARIATION OF TEMPERATURE IN GAS ZONES

As mentioned earlier, the temperatures in a gas zone are not assumed to be uniform over the zone. In reality, of course, the variation of gas temperature in the pipe will be continuous in each zone and from one zone to another. Thus, it is desirable to find a relation, in terms of the unknown zone-center temperatures, that will approximate the actual variation of gas temperature in the zones. The simplest approximation is to assume that the variation of emissive power in each zone is a two-dimensional linear function. Let the rectangular cross section of each zone be described by a rectangular coordinate system (ξ, η) whose origin is at the center of the zone cross section. Since the length of the cross section is $L/10$ and the width is $R/5$, the cross section is described by $-(L/20)\leq\xi\leq(L/20)$ and $-(R/10)\leq\eta\leq(R/10)$. The coordinate system (ξ, η) in the $(m,n)^{\text{th}}$ zone is oriented so that the positive direction is toward $\vec{R}_{i,j}$, the point in the $(i,j)^{\text{th}}$ zone that is being irradiated by the $(m,n)^{\text{th}}$ zone. The two-dimensional variation of emissive power in the cross section of the $(m, n)^{\text{th}}$ zone may then be given by

$$T^4(\xi,\eta)=T^4_{m,n}+(T^4_{m\pm1,n}-T^4_{m,n})\frac{\xi}{\xi_o}+(T^4_{m,n\pm1}-T^4_{m,n})\frac{\eta}{\eta_o} \quad (3)$$

where ξ_o and η_o are the length and width of the zone cross sections, respectively, and $T_{m\pm1,n}$ and $T_{m,n\pm1}$ are the temperatures at the centers of zones adjacent to the $(m,n)^{\text{th}}$ zone. The two-dimensional function given by equation (3) completely defines the temperature field throughout each of the toroidal gas zones, since the temperatures vary only in the cross sections of the zones and are otherwise circumferentially uniform because of the axisymmetry of the problem. Equation (3) is substituted for the emissive power T^4 in that integral of equation (2) which represents the radiation interchange between the surrounding gas zones and the center of the $(i, j)^{\text{th}}$ zone and is given as

$$\iiint \sigma T^4(\vec{r}_{m,n})f(\vec{r}_{m,n}-\vec{R}_{i,j})dv \quad (4)$$

Thus, this exchange integral may be expressed in terms of the unknown temperatures at the centers of the $(m,n)^{th}$ zone and two adjacent zones, and these temperatures may then be taken outside the integral sign. The details of evaluating the integral (eq. (4)) in terms of the unknown zone-center temperatures are given in appendix C.

EVALUATION OF EXCHANGE INTEGRALS

The labor of evaluating the gas-zone to gas exchange integrals (eq. (4)) and the other surface-zone to gas exchange integrals that appear in equation (2) is considerable, since these integrals are functions of the relative positions of the zones in question and the integrations have to be performed for each unique zone pair. Since the gas-zone to gas exchange integrals (eq. (4)) can be evaluated in terms of the zone-center temperatures, these temperatures may be taken outside the integral sign and the actual process of integration then becomes independent of temperature, as in the case of the surface-zone to gas integrals described earlier. In appendix B, it is shown that the form of the exchange factors $\vec{f(s)}$ is such that the volume integrals over the gas zones are transformed to surface integrals over the zone cross sections and the resulting integrations to be performed, which are described in appendix C, are of the form

$$\iint F[\vec{r}_{m,n}(\xi,\eta)-\vec{R}_{i,j}]\mathrm{d}\eta\,\mathrm{d}\xi \tag{5a}$$

$$\iint \xi F[\vec{r}_{m,n}(\xi,\eta)-\vec{R}_{i,j}]\mathrm{d}\eta\,\mathrm{d}\xi \tag{5b}$$

where $\vec{F(s)}=2\pi\rho\vec{f(s)}$ and ρ is the radius of the infinitesimal gas ring in the $(m,n)^{th}$ zone (see appendix C). Though a unique value of these integrals is associated with every zone pair (m,n) and (i,j), and there are $n^2=2500$ different gas-zone-pair combinations among the 50 zones, it is not necessary to compute 2500 separate integrals. This is true because use can be made of the symmetry created by the identical shape of the zones along the length of the pipe. The integrals in equations (5a) and (5b) are functions only of the respective radii of the $(m,n)^{th}$ and $(i,j)^{th}$ zones and their relative axial positions, or axial separations, since the size of the zones does not vary with axial position.

Thus, there are only $5\times5\times10=250$ unique gas-zone pairs and, consequently, the preceding integrations need only be performed 250 times instead of 2500. These integrals may then be evaluated by placing the $(i,j)^{th}$ gas zone at one end of the pipe in each of the five different radial positions and letting the $(m,n)^{th}$ gas zone range over all 50 zone positions in the pipe. In this way, all 250 (5×50) gas-zone to gas exchange integrals can be determined. The problem of the surface-zone to gas exchange integrals is handled in a similar manner. For the cylindrical wall-surface zones, there are a total of 500 different zone-pair combinations with the gas zones. Again, because the zones are of equal size along the length of the pipe, only 50 of these combinations are unique. The exchange integrals that correspond to these 50 unique combinations may then be evaluated by taking the wall-surface zone at one end of the pipe and letting the $(i,j)^{th}$ zone range over all 50 gas zones in the pipe. For the end-surface zone to gas exchange integrals, there are 250 possible zone-pair combinations all of which are unique. Since there are five radial end-surface zones and 50 gas zones ($5\times50=250$) no reduction in the number of exchange integrals is possible here.

The labor of evaluating these exchange integrals may be reduced considerably by making use of the following consideration. It is shown in appendix D of reference 1 that when the optical distance between two points in the gas is such that $\tau=k|\vec{s}|>7$, the error made in neglecting the radiant exchange between those points is less than 0.1 percent. Because of this, the exchange factors $\vec{f(s)}$ and $\vec{g(s)}$ may be set equal to zero for all $\tau>7$, and the evaluation of the exchange integrals at these distances is eliminated.

SOLUTION OF HEAT-BALANCE EQUATIONS

The evaluation of all the gas exchange integrals that appear in equation (2) having thus been described, the surface to gas exchange integrals become coefficients of the known surface emissive powers and the gas to gas exchange integrals become coefficients of the unknown gas-zone-center emissive powers in that equation. In this manner, all the coefficients of the gas-zone emissive powers in each of the 50 zone-center heat-balance equations of the form of equation (2) are determined. The finite sums over the gas zones in

equation (2) are therefore composed of linear combinations of these unknown emissive powers. Since the surface temperatures and heat sources are given parameters, the only unknowns left in this system of 50 equations are the 50 values of emissive power or temperature at the zone centers. In the absence of either flow or conduction, equation (2) will form a set of algebraic equations linear in the unknowns $\sigma T_{i,j}^4$ and may be solved directly by standard matrix methods for such problems. When either flow or conduction is present in the problem, however, the equations become nonlinear in $\sigma T_{i,j}^4$ as a result of the appearance of terms in temperature $T_{i,j}$, which arise from the derivative terms in equation (1). Consequently, the system of equations must then be solved by an iterative method for nonlinear algebraic equations such as the Newton-Raphson method.

It should be mentioned that the accuracy of the solution of these equations deteriorates rather rapidly when the zones themselves become optically dense, for instance, when the opacity of the zones in the direction of maximum heat transfer (radially) becomes greater than one mean free path ($\tau=1$). As the opacity increases, the solution of equation (2) is more susceptible to error because of the following two considerations: First, at high values of zone opacity, the assumption of linear variation of emissive power in the cross section of a zone is no longer necessarily an accurate representation of the actual situation, particularly in gas zones adjacent to a surface boundary. Second, as the zones become increasingly opaque, equation (2) tends to become indeterminate. This situation occurs when a zone becomes so opaque that an infinitesimal volume at the center of the zone effectively receives radiation only from the zone in which it is located and almost none from any of the surrounding zones. This has the following effect on the coefficients of the heat-balance equation (eq. (2)) for that particular zone. The exchange integrals from the other zones tend to vanish as the zones become opaque, and, consequently, so do the coefficients of the emissive powers of the other zones in the given equation. The exchange integral from the given zone to its center becomes larger, rapidly approaching the limiting value of 4, and thus cancelling out the emission coefficient at the zone center. Consequently, the coefficient of the emissive power of the given zone also tends to vanish. Therefore, since all the coefficients representing radiative exchange in equation (2) become vanishingly small, the effects of small errors made in numerical computation of the exchange integrals become magnified, and the system of equations also tends toward indeterminacy. Because of the previous considerations, use of the method of this report should be limited to cases in which the optical distance across the zone in the radial direction does not exceed one mean free path.

The application of the Newton-Raphson method to the solution of a system of nonlinear equations similar to the one just discussed is given in detail in appendix E of reference 1. The results of the solution of the system of equations (eq. (2)) are the 50 values of emissive power or temperature at the centers of the cross sections of the 50 gas zones. Since the temperature distribution of the gas in the pipe is continuous, the temperatures at the 50 gas-zone centers approximately determine the gas temperature distribution in the pipe. Although the temperature distribution in the pipe has thus been determined, the problem is not yet completely solved, since the heat exchange between the surfaces and the gas still remains to be found.

DETERMINATION OF HEAT TRANSFER TO SURFACE OF PIPE

The heat transfer to the surfaces of the pipe can be divided into two parts: (1) the direct radiant heat transfer between the surfaces themselves, and (2) the heat exchange between the surfaces and the gas. The transfer between the surfaces and the gas is also divided between that due to radiation and that due to conduction between the surface and the adjacent gas. The direct exchange between the surfaces is described by three different classes of exchange integrals. The first category is the exchange between two surface zones on the interior of the cylindrical wall:

$$q_{m\to i}=\sigma T_{w_m}^4 \int_{A_m}\int_{A_i} h_{ww}(\vec{r}_m-\vec{r}_i)\,dA_m\,dA_i \quad (6a)$$

Equation (6a) represents the radiation emitted from the m^{th} wall-surface zone that is absorbed at the i^{th} wall-surface zone. The exchange factor $h_{ww}(\vec{r}_m-\vec{r}_i)$ represents the radiant exchange between a wall-surface ring of infinitesimal width and area dA_m in position $\vec{r}_m$ on the m^{th}

wall-surface zone and a similar surface ring at position $\vec{r}_i$ in the i^{th} zone of area dA_i.

The second category of direct surface exchange is between two end-surface zones on opposite ends of the pipe. The following relation gives the emission from the n^{th} annular surface zone at one end to the j^{th} annular surface zone at the opposite end:

$$q_{n\to j}=\sigma T_{e_n}^4 \int_{A_n}\int_{A_j} h_{ee}(\vec{r}_n-\vec{r}_j)\,dA_n\,dA_j \qquad (6b)$$

The exchange factor $h_{ee}(\vec{r}_n-\vec{r}_j)$ represents the radiant exchange between an annular ring of infinitesimal width and area dA_n at position $\vec{r}_n$ in the n^{th} end-surface zone and a similar annular ring of area dA_j at position $\vec{r}_j$ in the j^{th} end-surface zone on the opposite end of the pipe. The final form of direct surface interchange is between an end-surface zone and a cylindrical wall zone. The following relation gives the emission from the m^{th} cylindrical surface zone on the wall to the j^{th} annular surface zone on an end:

$$q_{m\to j}=\sigma T_{w_m}^4 \int_{A_m}\int_{A_j} h_{we}(\vec{r}_m-\vec{r}_j)\,dA_m\,dA_j \qquad (6c)$$

The exchange factor $h_{we}(\vec{r}_m-\vec{r}_j)$ represents the radiant exchange between a wall-surface ring of infinitesimal width and area dA_m at position $\vec{r}_m$ in the m^{th} wall-surface zone and an annular surface ring of infinitesimal width and area dA_j at position $\vec{r}_j$ in the j^{th} end-surface zone. The derivation of the direct surface exchange factors h_{ww}, h_{ee}, and h_{we} is given in appendix B.

The evaluation of the radiation exchange between the gas and the surface is somewhat more involved. The discussion of the exchange between the gas and a wall-surface zone is similar to that between a gas zone and an end-surface zone; thus, for the sake of brevity, only the exchange between a gas zone and an end-surface zone is discussed.

At first, it would seem that the exchange between the gas and the surface could be given directly by the surface to gas exchange integrals that appear in equation (2). It should be emphasized, however, that those integrals are not for the exchange between an entire gas zone and a surface zone, but rather represent only the exchange between a surface zone and an infinitesimal volume located at the center of the cross section of a gas zone. Thus, the exact formulation for the exchange between the $(i, j)^{\text{th}}$ gas zone and the m^{th} wall-surface zone is given as

$$q_{(i,j)\to m}=\iint_{A_m} dA_m \iiint_{V_{i,j}} \sigma T^4(\xi,\eta)\,g_w(\vec{r}_m-\vec{r}_{i,j})\,dv_{i,j} \qquad (7a)$$

The integral represents exactly the radiation emitted from the entire $(i, j)^{\text{th}}$ gas zone that is transferred to the m^{th} surface zone.

Because of the high multiplicity of integration in equation (7a), the evaluation, as it stands, is prohibitively laborious. Consequently, to reduce this task to reasonable proportions, it is necessary to make another simplifying assumption. The assumption made is that the exchange integral from the gas zone to the surface zone can be approximated by the exchange integral from the gas zone to a point at the center of the surface zone; thus, the integration over A_m in the previous expression is eliminated. Therefore, the approximate expression for the emission from the $(i, j)^{\text{th}}$ gas zone to the m^{th} wall-surface zone becomes

$$q_{(i,j)\to m}=A_m \iiint_{V_{i,j}} \sigma T^4(\xi,\eta)\,g_w(\vec{R}_m-\vec{r}_{i,j})\,dv_{i,j} \qquad (7b)$$

where $\vec{R}_m$ is the position vector of the center of the m^{th} surface zone.

This approximation is quite good when the subject gas and surface zones are far apart; it is at its worst, though still acceptable, when the zones are adjacent if the dimensions of the gas zones are small in comparison with those of the pipe, as in the present case. The emissive-power distribution in the gas zone that appears in equation (7b) is again the linear approximation given by equation (3). It is shown in appendix B that, as for the case of $f(\vec{s})$, the form of $g(\vec{s})$ is such that the volume integral in equation (7b) reduces to a surface integral over the zone cross section. The details of the integration of equation (7b) are similar to those given in appendix C except that the emission is now to an infinitesimal surface ring at the center of the wall-surface zone instead of an infinitesimal volume at the center of the gas-zone

cross section, with an appropriate change in exchange factors from $\vec{f(s)}$ to $\vec{g_w(s)}$. Again, on the substitution of equation (3) for $T^4(\xi,\eta)$, equation (7b) is expressed in terms of the gas-zone-center temperatures, and the actual integration of the exchange factors becomes independent of temperature. In the same manner as discussed earlier for the case of the surface-zone to gas exchange integrals, it is necessary to compute only 50 unique values of the gas-zone to wall-surface exchange integrals arising from equation (7b). But for the gas-zone to end-surface exchange integrals, it is again necessary to compute values for all 250 different combinations.

The evaluation of radiant exchange to a surface zone from the gas zones and the other surface zones having been discussed, it is now possible to determine the net amount of heat transferred by radiation at each surface zone. As before, the procedure is similar for both cylindrical wall-surface zones and for end-surface zones, but for the sake of brevity only the procedure for cylindrical wall-surface zones will be discussed; the situation for the ends should then be self-evident. The equation that gives the net amount of heat transferred by radiation on the i^{th} wall-surface zone is

$$q_i=\sum_{m=1}^{10}\sigma T_{w_m}^4\int_{A_m}\int_{A_i}h_{ww}(\vec{r_m}-\vec{r_i})\,\mathrm{d}A_m\,\mathrm{d}A_i + \sum_{l=1}^{2}\sum_{n=1}^{5}\sigma T_{e_{l,n}}^4\int_{A_n}\int_{A_i}h_{we}(\vec{r_m}-\vec{r_i})\,\mathrm{d}A_n\,\mathrm{d}A_i + A_i\sum_{m=1}^{10}\sum_{n=1}^{5}\iiint_{V_{m,n}}\sigma T^4(\xi,\eta)\,g_w(\vec{r_{m,n}}-\vec{R_i})\,\mathrm{d}v_{m,n}-A_i\sigma T_{w_i}^4 \quad (8)$$

The first term in equation (8) represents the heat radiated to the i^{th} wall zones from all the other cylindrical wall zones, including the i^{th} zone. The second term represents the radiation transmitted from both ends of the cylinder to the i^{th} wall zone. The third term gives the radiation from all the gas zones that is received at the i^{th} surface zone. Finally, the last term represents the radiation emitted by the i^{th} wall-surface zone. If q_i, as given by equation (8), is positive, energy is being removed externally from the i^{th} surface zone, whereas if q_i is negative, energy must be supplied externally to the zone.

In the case of the ends of the cylinder, since the end surfaces are not really surfaces at all but are used merely as simple models of the radiation environment external to the ends of the cylinder, the heat-exchange equation for the end surfaces, which corresponds to equation (8), gives the net radiation heat transfer between the interior of the cylinder and the external environment.

The only other mode of heat transfer to the surfaces is conduction between the cylindrical wall surface and the adjacent gas zones. The conduction heat transfer at the cylindrical wall is given by

$$q_{c_i}=-A_i\lambda\left.\frac{\partial T}{\partial\rho}\right|_{\rho=\rho_o} \quad (9)$$

The temperature gradient in the gas at the wall $\rho=\rho_o$ is obtained numerically from the slope at the wall of a parabola fitted through the temperature of the subject wall-surface zone and the zone-center temperatures of the first and second gas zones away from the wall. In this way, the heat conducted at each wall-surface zone may be computed, and the result combined with that of equation (8) to obtain the net total heat transfer to the wall-surface zones.

PRACTICAL CONSIDERATIONS

In closing this section, several important practical aspects of the analysis herein should be emphasized. First, although allowance was made for continuous variation of gas temperature within he gas zones, the problem could still be stated solely in terms of the gas-zone-center temperatures. As a direct result of this circumstance, it becomes possible to perform the integration of the exchange integrals between zones in a manner independent of zone temperatures, or stated in another way, these exchange integrals are a function only of the shape of the cylinder, given by L/D, and of the opacity of the gas as given by $\tau_o=kD$. This consideration is extremely important, since the computation of these exchange integrals is much more time consuming than the solution of the remainder of the problem. Therefore, it makes sense to compute these exchange integrals separately for given values of L/D and kD, and to record the results in tabular form on punched cards or computer tape. In this manner, it is possible to solve the problem for a given cylinder and gas absorptivity for various boundary temperatures, sources in the gas, and flow rates with-

out the necessity of having to repeat the laborious computation of the exchange integrals each time.

RESULTS AND DISCUSSION

Equation (2) was solved on an IBM 7090 computer by using the methods described in the last section for the general case of a gray gas of uniform absorptivity enclosed in a black-walled cylindrical pipe with a length to diameter ratio of 5. Results were obtained for a range of optical diameter of the pipe, $\tau_o=kD$, between 0.2 and 10.0 and for a wide range of gas-flow rates and internal heat sources in the gas. For this particular geometry, it is difficult to present quantitative general results that give the effect of the interaction between conduction and radiation, as was done in reference 1. To obtain such results for a cylindrical geometry, it would be necessary to determine the combined radiative and conductive exchange in the annulus between two concentric cylindrical surfaces, a task that is beyond the scope of this report. Consequently most of the results presented are for radiant heating of a gas flowing through a cylindrical pipe. Results are presented, however, that give the effect of thermal conduction on heat transfer from isothermal pipe walls to a flowing absorbing gas, and the effect of combined radiative and conductive transfer from a heat-generating cylindrical core of gas in the center of the pipe through an absorbing gas to the pipe wall is also briefly investigated.

RADIANT HEAT TRANSFER FROM PIPE WALLS TO FLOWING GAS

In the subsequent discussion, the gas enters the pipe at one of the ends at a uniform temperature T_i and the temperature of the corresponding end surface, which represents the external environment at the pipe inlet, is made uniformly equal to this incoming gas temperature. The temperature of the cylindrical wall of the pipe T_* is uniform along the length of the pipe and is greater than T_i. The end-surface temperature at the outlet of the pipe is assumed uniform over that end surface and is made equal to the mean mixed gas exit temperature T_o. This is somewhat of an approximation, since although the gas enters the pipe at a uniform temperature, the gas temperature at the outlet will not generally be uniform in the radial direction. It is assumed, however, that temperature equilibrium in the gas is attained shortly after the gas leaves the pipe, and since the end surface at the outlet represents the environment external to the outlet of the pipe, the assumption is considered reasonable.

In order to obtain the results in the most general form, it is necessary to present them in terms of dimensionless parameters. When equation (1) is divided by $\sigma k T_*^4$ and the internal heat-generation term is neglected, the equation is reduced to dimensionless terms as follows:

$$4\left(\frac{T}{T_*}\right)^4+\frac{Gc_p}{\tau_o\sigma T_*^3}\frac{\partial\left(\frac{T}{T_*}\right)}{\partial\left(\frac{x}{D}\right)}-\frac{\left(\frac{\lambda}{D}\right)}{\tau_o\sigma T_*^3}\frac{1}{\left(\frac{\rho}{D}\right)}\frac{\partial}{\partial\left(\frac{\rho}{D}\right)}\left[\left(\frac{\rho}{D}\right)\frac{\partial\left(\frac{T}{T_*}\right)}{\partial\left(\frac{\rho}{D}\right)}\right]=\int\int\int\left(\frac{T}{T_*}\right)^4 f(\vec{s})\,dv+\int\int\left(\frac{T}{T_*}\right)^4 g(\vec{s})\,dA$$

The integrals on the right, as stated in the analysis, may be represented as functions of τ_o and L/D. Therefore, the solution to the preceding dimensionless equation is determined uniquely by the parameters $Gc_p/\tau_o\sigma T_*^3$, $(\lambda/D)/\tau_o\sigma T_*^3$, τ_o, L/D, and the boundary condition at the pipe inlet:

$$\left.\frac{T(x/D,\,\rho/D)}{T_*}\right|_{(x/D)=0}=\frac{T_i}{T_*}$$

If the dual dependence of τ_o in the parameter group is eliminated, the dimensionless results for heat transfer to a flowing gas may be presented uniquely in terms of the parameters $Gc_p/\sigma T_*^3$, $(\lambda/D)/\sigma T_*^3$, τ_o, and L/D. The dimensionless parameter $Gc_p/\sigma T_*^3$ is known as the Boltzmann number N_{BO} and is used in both references 1 and 2 in the discussion of radiant heat transfer to flowing gases. The dimensionless parameter $(\lambda/D)/\sigma T_*^3$ is the radiation-conduction parameter N_{CR} and is used to represent the effects of thermal conduction on heat transfer in a radiation-absorbing gas.

Results for radiant transfer to a flowing gas in the pipe, with conduction transfer neglected ($N_{CR}=0$), are given in figure 4, for the case of slug flow of the gas, the flow rate G being uniform over the pipe cross section. As will be seen later, it may be a reasonable assumption to neglect conduction transfer when the temperature level in the

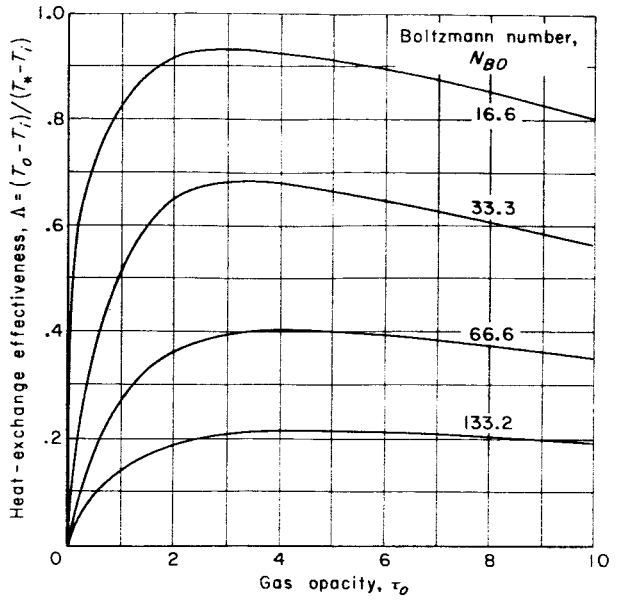

FIGURE 1.—Heat transfer to absorbing gas flowing through pipe from isothermal pipe walls for slug flow without conduction. Ratio of gas inlet to wall temperature, 0.4; length to diameter ratio, 5; conduction-radiation parameter, 0.

gas becomes very high. The parameter $\Lambda = (T_o - T_i)/(T_* - T_i)$ represents the effectiveness of the radiant heat transfer to the gas. It is the ratio of the actual heat transfer to the gas to the maximum heat transfer theoretically possible. The value of T_o in the expression for Λ is the mixed-mean gas temperature at the outlet of the pipe.

The results given in figure 4 are very similar to those obtained in reference 1 for radiant heat transfer to a gas flowing between two parallel flat plates. As the absorptivity of the gas, and thus τ_o, increases from zero, the amount of energy radiated from the wall of the pipe that is absorbed by the gas increases from zero to some maximum value. Thereafter, for further increases in gas absorptivity, the amount of heat transferred to the gas steadily decreases. The reason for this eventual decrease in heat transfer with increasing gas absorptivity is caused by the self-shielding of the gas as it becomes more absorptive. At high values of gas absorptivity, most of the direct radiation from the wall of the pipe is absorbed in the gas adjacent to the wall, and since it is re-emitted isotropically in the gas, about one-half is remitted toward the wall and reabrorbed there. Therefore, very little direct wall radiation reaches the gas in the center of the pipe and consequently the gas there remains relatively cool. As the gas absorptivity increases, the layer of gas adjacent to the wall required to attenuate the direct wall radiation becomes thinner; consequently, a greater proportion of the gas in the pipe is shielded from the direct wall radiation, which results in lower overall heat transfer.

The effects of conduction and velocity profile on the heat transfer to a flowing gas are shown in figures 5(a) and (b) for $N_{BO}=33$. The results in figure 5(a) are for a slug velocity profile, as in the case of those presented earlier in figure 4, whereas the results for a parabolic velocity distribution are shown in figure 5(b). For the case of the parabolic velocity distribution, the Boltzmann number is based on the average flow rate in the pipe. Obviously, the effect of added conduction is always to increase the overall heat transfer to the gas. It is interesting to note, however, what the relative effects of conduction on the overall heat transfer are. In figures 3(a) and (b), the values of Λ at $\tau_o=0$ represent the thermal effectiveness of heat exchange due to conduction alone and, thus, represent a "floor" under the curves as τ_o increases and radiant transfer becomes effective. It is seen that for values of $N_{CR}=(\lambda/D)/\sigma T_*^3<0.05$, radiation seems to be the dominant mode of transfer except, of course, at very low values of τ_o where conduction is always dominant; however, for values of $N_{CR}>0.5$, the transfer appears to be primarily by conduction for all values of τ_o. Thus, if the value of N_{CR} in a particular situation is known, the mode of heat transfer that will be dominant in the combined process can be quickly ascertained. Although the thermal conductivity of most gases increases slightly with temperature, N_{CR} is also inversely proportional to the cube of the temperature. Therefore, the effect of conduction transfer in a radiation-absorbing gas decreases rapidly as the temperature level becomes high, since the value of N_{CR} drops very quickly despite the increase in thermal conductivity. The results shown for a parabolic velocity profile in figure 5(b) are very similar to those shown in figure 5(a), except that for any given value of N_{CR}, the values of Λ are less than the corresponding values for a slug velocity profile. This decrease in Λ is to be expected, since a parabolic-velocity profile presents a much smaller heat sink adjacent to the wall than a slug-velocity profile does.

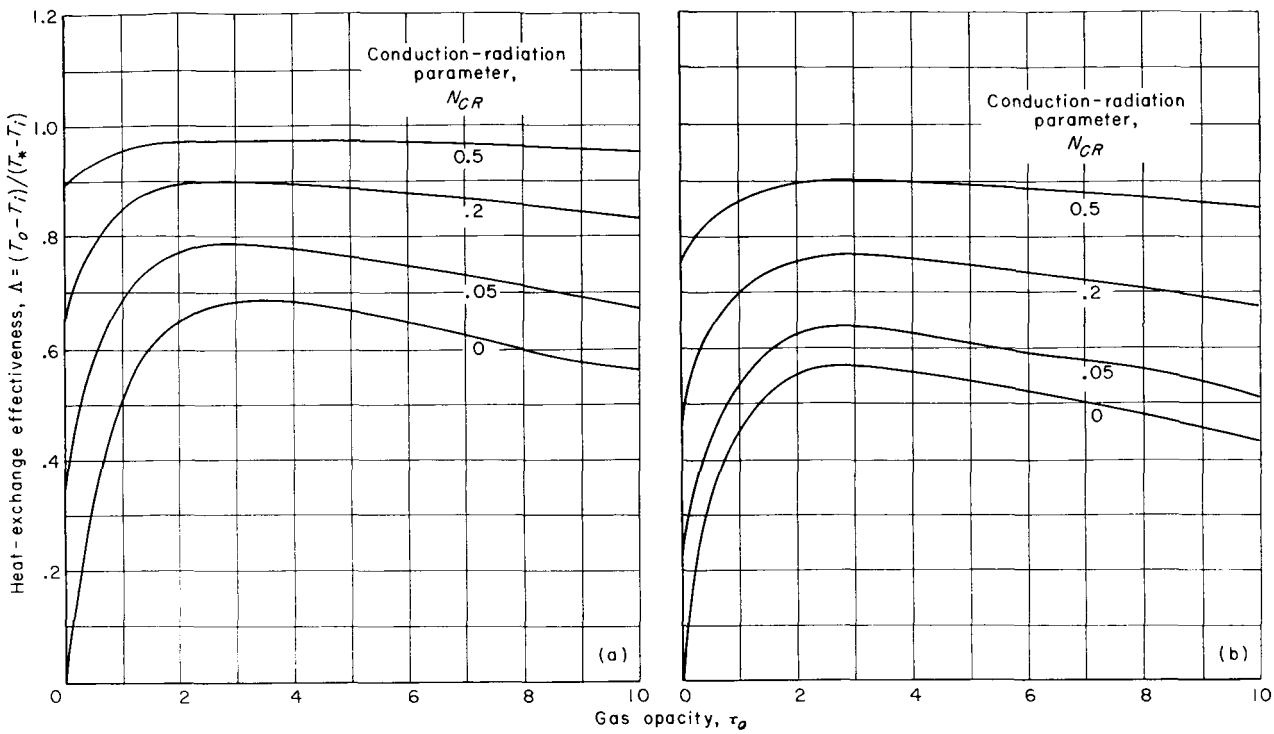

(a) Slug velocity profile.
(b) Parabolic velocity distribution.

FIGURE 5.—Heat transfer to absorbing gas flowing through pipe from isothermal pipe walls with combined radiation and conduction. Ratio of gas inlet to wall temperature, 0.4; length to diameter ratio, 5.0; Boltzmann number, 33.

RADIANT HEAT TRANSFER FROM UNIFORMLY HEATED CYLINDRICAL GASEOUS CORE TO SURROUNDING FLOWING GAS AND PIPE WALL

The situation discussed here is typical of radiant heat transfer from an electric arc, plasma jet, or gaseous-reactor core enclosed in a pipe to the walls of the pipe and to the gas flowing in the annulus between the core and the pipe. For the results presented, the radius of the heat-generating gaseous core is equal to 0.2 of the pipe radius, the heat-generation rate per unit volume is uniform both axially and radially in the core, and the absorption coefficients of the core and the surrounding gas are equal. The boundary conditions are similar to those used in the preceding section. The gas enters the pipe at a uniform temperature T_i and this temperature is again taken to be uniform over the end surface of the inlet of the pipe. The wall temperature of the pipe is uniform along the length of the pipe and is also taken to be equal to T_i, the gas-inlet temperature. The end-surface temperature at the outlet of the pipe is assumed to be uniform over that surface and is again made equal to the mean mixed gas temperature at that end. The effects of thermal conductivity are again neglected, and the results presented are for the case of slug flow of the gas. Although the temperature of the heat-generating core in the center of the pipe is much hotter than that of the surrounding gas, the assumption of uniform temperature on the ends of the pipe is not unreasonable, because the cross-sectional area of the core is such a small fraction of the total end area. The ratio of the mixed mean gas-outlet temperature to gas-inlet temperature is used as a parameter in presenting the results. In order to keep this temperature ratio fixed for a number of different cases, it is necessary to vary the amount of heat generation in the core accordingly.

Since, in the case of an electric arc or gaseous reactor enclosed in a pipe, the temperature of the plasma is usually much hotter than the melting point of the material from which the pipe is fabricated, it is necessary to cool the enclosing pipe externally when a large fraction of the heat generated in the plasma is deposited directly on the pipe walls. The radiant heat transfer from the

plasma to the pipe walls may be attenuated, however, by increasing the flow rate and opacity of the gas in the annulus between the plasma core and the pipe wall. Consequently, the results for this configuration will be presented in the form of fractional heat load to the wall as a function of temperature-rise ratio of the gas flowing through the pipe, Boltzmann number (indicative of gas flow rate), and gas opacity. Figure 6 gives the fraction of heat generated that is absorbed by the pipe wall as a function of Boltzmann number, with gas opacity τ_o as a parameter for a fixed value of gas-temperature ratio in the pipe. As expected, an increase in the gas flow rate decreases the amount of heat transmitted to the wall of the pipe for all values of gas absorptivity. Also, the effectiveness of increasing the absorptivity in reducing the heat load on the wall increases as the Boltzmann number increases. Thus, at low values of Boltzmann number (low values of gas flow), the percent of heat absorbed by the wall is affected only slightly by changes in gas absorptivity; however, at higher Boltzmann numbers, the percent of absorption at the wall decreases rapidly as the gas opacity increases. The percent of absorption at the wall decreases continuously with increasing gas flow but seems to approach a limiting value that is a function only of the opacity of the gas in the pipe. This limiting value of percent absorption at the wall decreases with increasing gas opacity and is less than 4 percent for values of gas opacity τ_o greater than 10. Figure 7 is essentially a cross plot of figure 6 that shows more clearly the effect of gas opacity on the heat load to the wall. As mentioned earlier, at low values of

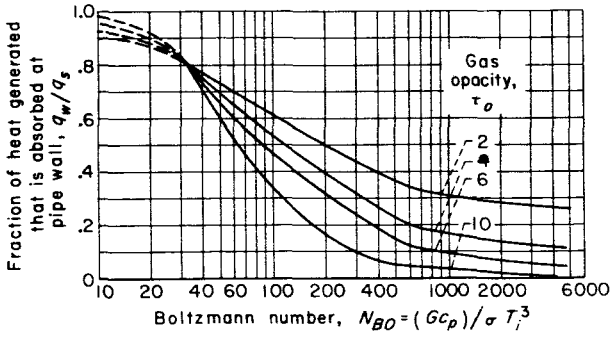

FIGURE 6.—Heat load to pipe wall as function of Boltzmann number based on wall temperature for various values of gas opacity. Wall temperature equal to gas inlet temperature; length to diameter ratio, 5; temperature rise ratio, 2.

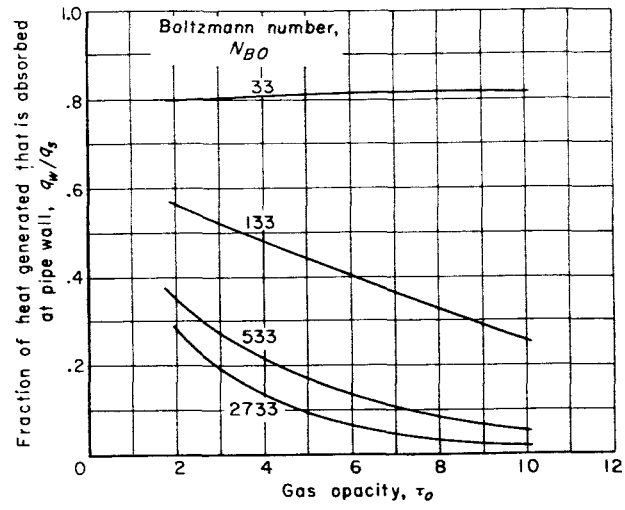

FIGURE 7.—Fractional heat load to wall from heat-generating gaseous core as function of gas opacity for several values of Boltzmann number based on gas inlet temperature. Wall temperature equal to gas inlet temperature; temperature rise ratio, 2; length to diameter ratio, 5.

Boltzmann number, the opacity of the gas has practically no effect on the percent heat load to the wall. As the flow rate in the pipe is increased however, an increase in the gas absorptivity causes the heat load to the wall to decrease rapidly. Also for very large Boltzmann numbers, a limit is reached where the heat load to the wall becomes a function only of gas opacity and is nearly independent of further increases in flow rate.

Figure 8 shows the effect of varying the temperature-rise ratio of the gas flowing in the pipe. As expected, when the temperature-rise ratio of the gas in the pipe increases, a large fraction of the heat generated is lost to the wall. From the fore-

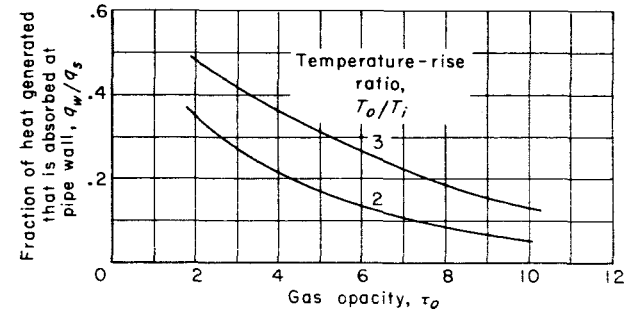

FIGURE 8.—Fractional heat load to wall at constant Boltzmann number of 533, based on gas inlet temperature, as function of gas opacity for two values of temperature rise ratio. Length to diameter ratio, 5.

going discussion it appears that in order to shield a pipe wall from the radiation of a hot arc or plasma enclosed in the pipe, it is necessary not only to make the intervening gas stream relatively opaque but also to make the gas flow rate sufficiently large to maintain a high value of Boltzmann number. The specific results obtained here were for a pipe with a length to diameter ratio of 5, which had a heat-generating gaseous core at the center whose radius was 0.2 that of the pipe. Though the quantitative results for this case probably do not apply to other pipe configurations, it is expected that the qualitative trends will be the same.

RADIANT HEAT TRANSFER FROM A UNIFORMLY HEATED CYLINDRICAL GASEOUS CORE THROUGH AN ABSORBING STAGNANT GAS TO THE PIPE WALL

The situation here is much the same as for the previous case except that the absorbing gas between the gaseous heat-generating core and the walls is stationary. The cylindrical wall of the pipe and the two end surfaces are kept at the same uniform temperature. Consequently, since there is no flow and the conditions at both ends of the pipe are the same, if the end effects are small, the conditions at the middle of the cylinder are essentially the same as those in a similar pipe of infinite length. It was found that for $L/D=5$ the end effects were relatively small, and the principal variation of temperature in the pipe was in the radial direction. The axial variations of temperature in the pipe were small and due only to the presence of the finite ends of the pipe.

For the case of no conduction or flow in the pipe, equation (1) becomes linear in the emissive power $E=\sigma T^4$, and the results are best presented by illustrating the dimensionless emissive-power profiles in the gas. Because of the linear nature of the problem, the emissive-power difference between points in the gas and the wall is directly proportional to the radial heat flux transmitted from the gaseous core to the pipe walls. Thus, the results may be made dimensionless by dividing this difference of emissive powers by the radial heat flux measured at a radius ratio of 0.2 at the edge of the gaseous core. The radial heat flux at this point is obtained by dividing the total heat generation in the core $q'''\pi D^2L/4$ by the core surface area πDL. Thus, the radial flux at this radius is $q''=q'''D/4$. The results could have been made dimensionless just as well by dividing ΔE by the heat flux at any other radius in the pipe outside the gaseous core, for instance, by the flux at the wall. Because there are no sources outside the gaseous core, the radial heat flux varies inversely with the radius, and the heat fluxes at any two radial stations differ only by a constant factor equal to the ratio of the two radii. Thus, the present choice is purely arbitrary.

The results are shown in figure 9 for various values of gas opacity. The discontinuity in the emissive-power profiles at $\rho/\rho_o=0.2$ is due to the radial step change in internal heat generation at that point in going from the gaseous heat-generating core to the surrounding gas. Since conduction is not present, there is no reason for the emissive-power profile to be continuous at that point or at

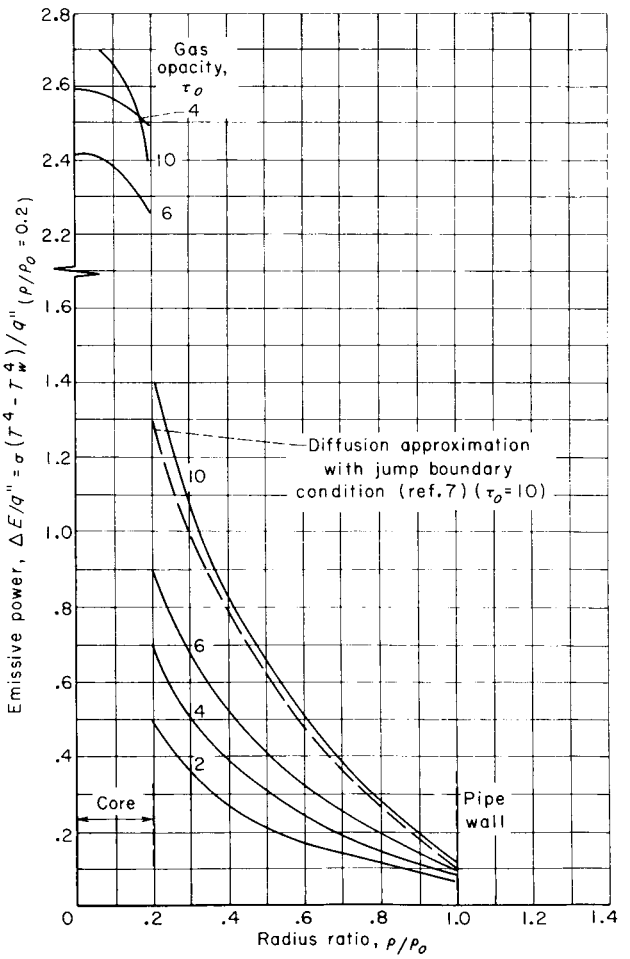

FIGURE 9.—Dimensionless radial emissive power distribution for radiation from gaseous heat-generating cylindrical core through annulus of stationary absorbing gas to black cylindrical pipe wall for various values of gas opacity.

the wall where $\rho/\rho_o=1$. The discontinuity of emissive-power profiles at gas-surface or source boundaries is a well-known phenomenon associated with pure radiation transfer in absorbing gases. As seen from figure 9, with increasing gas opacity, the emissive-power curves in the region outside the core become higher and steeper, as expected, since an increase in the opacity increases the resistance to heat transfer. At the same time, however, the emissive power of the heat-generating gas in the core at first decreases with increasing absorptivity to some minimum value and then increases again slightly with further increases in opacity. The reason for this behavior in the core is that the emission from a gaseous volume source is roughly proportional to the product of its absorption coefficient with the emissive power of the source relative to its surroundings. This relation does not hold exactly for finite volumes of gases because of self-shielding in the volume, but it is still qualitatively correct. Consequently, for the same amount of energy emitted, as the absorptivity in the core increases, as indicated by increased opacity of the gas in the pipe, the relative emissive power, as indicated by the jump in emissive power at the core boundary, decreases. The rise in dimensionless emissive power in the core in going from a gas opacity of $\tau_o=6$ to $\tau_o=10$ is believed to be a result of the fact that in that range of τ_o although the jump in emissive power at the core boundary decreases as described previosuly when the opacity τ_o increases from 6 to 10, the increase in emissive power in the gas outside the core is even more rapid, which results in a net increase of the emissive-power level in the core.

Also plotted in figure 9 for $\tau_o=10$, is the approximate emissive-power profile of an absorbing gas in an annulus between two concentric cylindrical surfaces. These results were obtained from an analysis derived in reference 7 based on the Rosseland diffusion approximation with a jump boundary condition. Although the analysis of reference 7 postulates an inner cylindrical surface rather than a gaseous core as the radiation source, the results apply equally well to the present case between the core and the wall, since the gaseous core may be replaced by a diffusely emitting cylindrical surface that has the same shape and size as the core, and whose emissive power is such that the net radiant flux given off by this surface is equal to that emitted from the gaseous core. The agreement of the results based on the analysis in reference 7 with those obtained in this report is fairly good, especially considering the fact that the Rosseland approximation with a jump boundary condition is valid only for high values of gas opacity. The gas opacity of $\tau_o=10$ for which the results are compared is about the lower limit for the validity of that analysis.

The effect of conduction on the radial temperature profile in the gas for the previous configuration is shown in figure 10. Because equation (1) becomes nonlinear in the presence of conduction, it is no longer possible to present the dimensionless results that show the effect of conduction in the same parametric form that was used to portray the pure radiation results in figure 9. The conduction-radiation parameter $N_{CR}=(\lambda/D)/\sigma T_*^3$, which was derived earlier, is again used to present

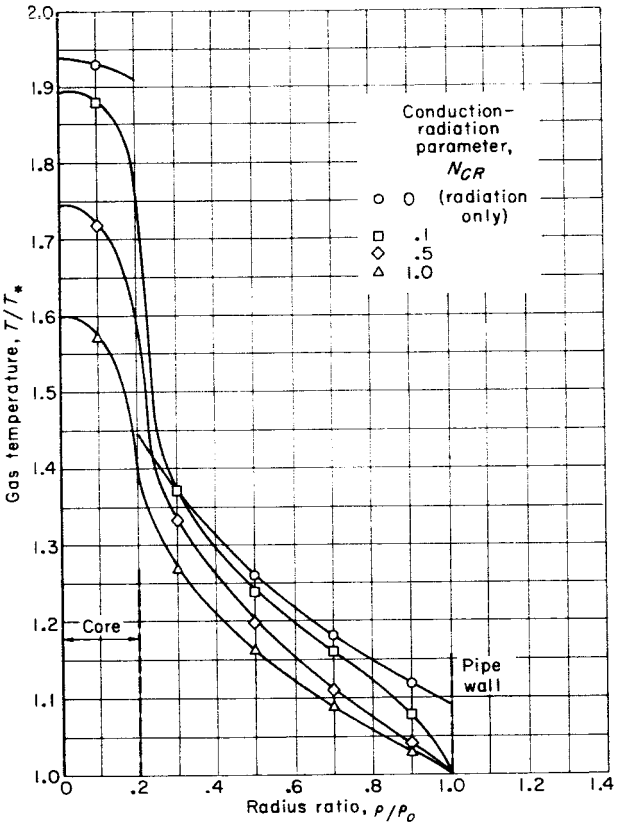

FIGURE 10.—Dimensionless temperature profiles for emission from gaseous heat-generating cylindrical core through annulus of stationary absorbing, conducting gas to black cylindrical pipe wall showing effect of conduction in gas. Gas opacity, 4.0; dimensionless radial heat flux, 5.0.

the results in the presence of conduction. The surface temperature of the cylindrical wall is taken as the reference temperature T_*. The radial heat flux q'' at $\rho/\rho_o=0.2$ is made dimensionless by dividing by σT_*^4. Consequently, for this case, the results for combined conduction and radiation depend uniquely on the dimensionless parameters N_{CR}, $q''/\sigma T_*^4$, and τ_o. The effect of L/D is omitted here, because, as before, only one-dimensional radial temperature profiles at the middle of the pipe are considered, and for L/D sufficiently large, its effect is merely a perturbation on the results. Thus, the results in figure 10 give the dimensionless temperature profiles of the gas in the pipe for several values of N_{CR} and for fixed values of τ_o and $q''/\sigma T_*^4$. The results are not unusual. With conduction, the temperature profiles become continuous at the core boundary and at the wall, and the overall temperature level in the pipe, especially in the core, is reduced since the added conduction increases the overall heat transfer.

CONCLUDING REMARKS

The method of this report for solving the problem of radiant heat transfer to an absorbing gas in a circular pipe under the influence of flow and conduction closely parallels that given in reference 1 for solving essentially the same problem in a channel formed by a pair of semi-infinite flat plates. Results were presented for a gray gas of uniform absorptivity enclosed in a black circular pipe with a length to diameter ratio of 5.

For the case of radiant heat transfer from isothermal walls of the pipe to a cooler, flowing, absorbing gas, the heat transfer to the gas goes through a maximum as the opacity of the gas is increased. The maximum heat transfer occurred in the range of gas opacity from 3 to 4. This effect is due to the self-shielding of the gas to the radiation being emitted from the pipe walls and was also observed in reference 1 in heating an absorbing gas flowing between two isothermal flat plates.

The effect of thermal conduction on heat transfer to a flowing radiation-absorbing gas becomes important whenever the conduction-radiation parameter N_{CR} exceeds 0.05 or whenever the gas opacity is less than 1. As the temperature level of the gas rises, although the thermal conductivity of the gas will generally increase somewhat, conduction rapidly becomes relatively less important than radiation. This decrease in importance is due to the inverse variation of N_{CR}, which results in the rapid decrease in the value of this parameter as the temperature rises despite the attendant increase in thermal conductivity of the gas.

When a heat-generating gaseous core is contained in the pipe, as in the case of a plasma jet or in the coaxial-jet gaseous nuclear-rocket concept, a practical problem of current interest is to prevent melting or burnout of the pipe wall by shielding it from the radiation emitted by the high-temperature plasma core. It was shown herein that, if the opacity of the gas in the pipe is greater than 10, the heat load to the wall of the pipe can be made negligibly small if, in addition, the gas flow rate is such that the Boltzmann number in the pipe, based on the wall temperature, becomes 1000 or greater. On the basis of these results, it is felt that a device in which a high-temperature plasma must be contained, such as a gaseous nuclear rocket, is feasible from a heat-transfer standpoint if a gas opacity of approximately 10 is attainable over the temperature range of interest.

Results are also presented for one-dimensional radial radiant heat transfer from a heat-generating cylindrical gaseous core to the pipe walls. The emissive-power profile in the gas between the core and the wall was compared with results from reference 7 for an absorbing gas in an annulus between two concentric black cylindrical surfaces, and agreement was found to be good. For the case where no conduction was present, a large jump in emissive power occurred at the core boundary. The magnitude of the jump was roughly inversely proportional to the opacity of the gas. In the presence of conduction, the jump disappears, and the radial-temperature profile becomes continuous. As the conductivity of the gas is increased from zero, the temperature levels in the gas, especially in the core, rapidly decrease as expected.

LEWIS RESEARCH CENTER
NATIONAL AERONAUTICS AND SPACE ADMINISTRATION
CLEVELAND, OHIO, *September 25, 1962*

Appendix A

SYMBOLS

A	surface area
c_p	specific heat of gas
D	diameter of pipe
dV	infinitesimal volume located at center of gas-zone cross section
dv	arbitrary infinitesimal gas volume
E	emissive power, σT^4
$\vec{F(s)}$	gas-ring-source to gas radiation exchange factor per unit cross-sectional area of ring $\vec{F(s)}=2\pi\rho\vec{f(s)}$
$\vec{f(s)}$	gas-ring-source to gas radiation exchange factor per unit volume of ring
G	flow density of gas, weight flow per unit area
$\vec{g(s)}$	surface-ring-source to gas radiation exchange factor
$\vec{h(s)}$	surface-ring-source to surface radiation exchange factor
I	integral function (see eq. (B10))
k	radiation absorption coefficient of gas, reciprocal length
N_{BO}	Boltzmann number, $Gc_p/\sigma T_*^3$
N_{CR}	conduction-radiation parameter, $(\lambda/D)/\sigma T_*^3$
q	heat transferred to surfaces
q''	radial heat flux per unit area
q'''	heat generation per unit volume of distributed sources in gas
$\vec{R}$	position vector of zone center in interior of pipe or on its surface
$\vec{r}$	position vector of arbitrary point in interior of pipe or on its surface
$\vec{r_o}$	position vector of gas volume dV in interior of pipe
$\vec{s}$	relative position vector between two points in pipe
T	temperature
x	axial coordinate
β	arbitrary function (see eq. (B8g))
η	coordinate in radial direction in cross section of gas zone
η_o	radial width of cross section of gas zone
θ	angular coordinate
Λ	heat-exchange effectiveness, $(T_o-T_i)/(T_*-T_i)$
λ	thermal conductivity of gas
ξ	coordinate in axial direction in cross section of gas zone
ξ_o	length of gas zone cross section
ρ	radius of point in interior of pipe
ρ_o	radius of pipe
σ	Stefan-Boltzmann constant
τ	optical distance between two points in pipe, $\tau=k\lvert\vec{s}\rvert$
τ_o	optical diameter of pipe or opacity of gas, $\tau_o=kD$

Subscripts:

C	conduction
e	end surface of pipe
i	position along length of pipe of fixed gas or wall-surface zone (usually that on which heat balance is taken), $i=1, 10$
in	conditions at inlet of pipe
j	radial position of fixed gas or end-surface zone in pipe measured from center of pipe outward (usually for that zone on which heat balance is taken), $j=1, 5$
l	end number, $l=1, 2$
m	general position along length of pipe of gas or wall-surface zone, $m=1, 10$
n	general radial position from center of pipe to wall of gas or end-surface zone, $n=1, 5$
o	integrated mean conditions at outlet of pipe
R	radiation
s	surface
w	inner surface of pipe wall
$*$	reference temperature

APPENDIX B

DERIVATION OF EXCHANGE FACTORS FOR CYLINDRICAL GEOMETRY

GAS TO GAS EXCHANGE FACTORS

Since the conditions in the cylinder are axisymmetric, the conditions in a ring of gas at a given radius from the center of the cylinder will be uniform. Thus, it is sufficient to consider the exchange between such a ring of gas of infinitesimal cross section and an infinitesimal volume at some other point in the cylinder. This situation is shown in sketch (a). The radius of the ring of

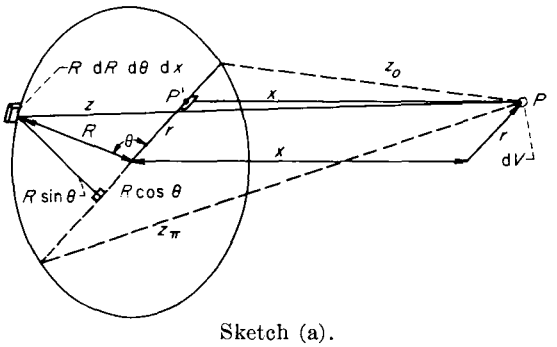

Sketch (a).

gas is R and the infinitesimal volume at P, to which this ring radiates, is at axial distance x from the plane of the ring and at some radius r from the centerline. The distance from P to some point on the ring is given by z. Let the emissive power of the ring be unity and let dV be the infinitesimal volume at P. Consider the radiation from an infinitesimal arc of the ring that is transmitted to and absorbed at P. Since the volume of this infinitesimal arc is $R\,dR\,d\theta\,dx$, the radiation from this arc that is absorbed at P is

$$dq_P=\frac{4kR\,dR\,d\theta\,dx}{4\pi z^2}\,e^{-kz}k\,dV \qquad \text{(B1)}$$

Let P' be the projection of P on the plane of the ring and let θ be the angle between the radius vector through P' and the radius vector to the radiating arc on the ring. The distance z can then be found from the relation

$$z^2=x^2+(r-R\cos\theta)^2+R^2\sin^2\theta \qquad \text{(B2)}$$

If equation (B1) is integrated from $\theta=0$ to 2π, the contribution of the entire ring to the absorption at P is obtained. Note from equation (B2) that the integrand given by equation (B1) is symmetrical about $\theta=\pi$; thus

$$\delta q_P=2k^2\,dV\,\frac{R}{\pi}\,dR\,dx\int_0^\pi\frac{e^{-kz}}{z^2}\,d\theta \qquad \text{(B3)}$$

where the relation between z and θ is given by equation (B2). As the situation stands, z, and thus the integral in equation (B3), is a function of the three parameters x, r, and R. Since the integral in equation (B3) must be evaluated numerically and then tabulated for use in the zone exchange-integral computations, it is important to reduce its functional dependence to as few distinct variables as possible. The expansion of equation (B2) results in

$$z^2=x^2+R^2+r^2-2Rr\cos\theta \qquad \text{(B4)}$$

Define

$$z_o^2=z^2(0)=x^2+R^2+r^2-2Rr$$
$$z_\pi^2=z^2(\pi)=x^2+R^2+r^2+2Rr \qquad \text{(B5)}$$

thus,

$$x^2+R^2+r^2=\frac{z_o^2+z_\pi^2}{2} \qquad \text{(B6)}$$

and

$$2Rr=\frac{z_\pi^2-z_o^2}{2} \qquad \text{(B7)}$$

Substitution of these relations into equation (B4) results in

$$z^2=\frac{z_o^2+z_\pi^2}{2}+\frac{z_o^2-z_\pi^2}{2}\cos\theta \qquad \text{(B8a)}$$

Thus, as given by equation (B8a), z is now a function of only two parameters, z_o and z_π. If, in addition, the substitution $\tau=kz$ is made, equation (B3) may be now also expressed in terms of the two parameters τ_o and τ_π. The expression for $d\theta$ in equation (B3) is found in terms of $d\tau$ as follows: Write equation (B8a) in terms of τ and differentiate to obtain

$$2\tau\,d\tau=-\frac{\tau_o^2-\tau_\pi^2}{2}\sin\theta\,d\theta \qquad \text{(B8b)}$$

Solve equation (B8a) for cos θ to obtain

$$\cos\theta=\frac{2\tau^2-(\tau_o^2+\tau_\pi^2)}{\tau_o^2-\tau_\pi^2} \tag{B8c}$$

Then substitute

$$\sin\theta=\sqrt{(1-\cos\theta)(1+\cos\theta)} \tag{B8d}$$

into equation (B8c) to obtain

$$\sin\theta=\frac{-2}{\tau_o^2-\tau_\pi^2}\sqrt{(\tau^2-\tau_o^2)(\tau_\pi^2-\tau^2)} \tag{B8e}$$

Substitute this result in equation (B8b) to obtain

$$d\theta=\frac{2\tau\,d\tau}{\sqrt{(\tau^2-\tau_o^2)(\tau_\pi^2-\tau^2)}} \tag{B8f}$$

Define

$$\beta\left(\frac{\tau}{\tau_o}\right)=\frac{2\left(\frac{\tau}{\tau_o}\right)}{\sqrt{\left[\left(\frac{\tau}{\tau_o}\right)^2-1\right]\left[\left(\frac{\tau_\pi}{\tau_o}\right)^2-\left(\frac{\tau}{\tau_o}\right)^2\right]}} \tag{B8g}$$

then

$$d\theta=\beta\left(\frac{\tau}{\tau_o}\right)\frac{d\tau}{\tau_o} \tag{B8h}$$

and

$$\delta q_P=2k^4\,dV\frac{R}{\pi}\,dR\,dx\int_1^{\tau_\pi/\tau_o}\frac{e^{-\tau}}{\tau^2}\beta\left(\frac{\tau}{\tau_o}\right)d\left(\frac{\tau}{\tau_o}\right) \tag{B9}$$

By examining equation (B4) and converting to a function of τ, it becomes obvious that τ_o and τ_π are precisely the minimum and maximum optical distances, respectively, from the ring to point P. If $f(\vec{s}-\vec{P})$ is defined as the exchange factor between the gas ring through $\vec{s}$ of infinitesimal volume $2\pi R\,dR\,dx$ and the infinitesimal volume dV at $\vec{P}$, then the radiant exchange between those two volumes is given by

$$\delta q=(2\pi R\,dR\,dx)(k\,dV)f(\vec{s}-\vec{P})$$

Then, in terms of equation (B9), $f(\vec{s}-\vec{P})$ becomes

$$f(\vec{s}-\vec{P})=f\left(\tau_o,\frac{\tau_\pi}{\tau_o}\right)$$

$$=\frac{k^3}{\pi^2}\frac{e^{-\tau_o}}{\tau_o^2}\int_1^{\tau_\pi/\tau_o}\frac{e^{-(\tau-\tau_o)}}{\left(\frac{\tau}{\tau_o}\right)^2}\beta\left(\frac{\tau}{\tau_o}\right)d\left(\frac{\tau}{\tau_o}\right) \tag{B10}$$

The parameterization here is changed to $\left(\tau_o,\frac{\tau_\pi}{\tau_o}\right)$ because this is the most convenient form for tabular representation of the integral in equation (B10). The function

$$I_1\left(\tau_o,\frac{\tau_\pi}{\tau_o}\right)=\int_1^{\tau_\pi/\tau_o}\frac{e^{-(\tau-\tau_o)}}{\left(\frac{\tau}{\tau_o}\right)^2}\beta\left(\frac{\tau}{\tau_o}\right)d\left(\frac{\tau}{\tau_o}\right) \tag{B11}$$

is plotted in figure 11.

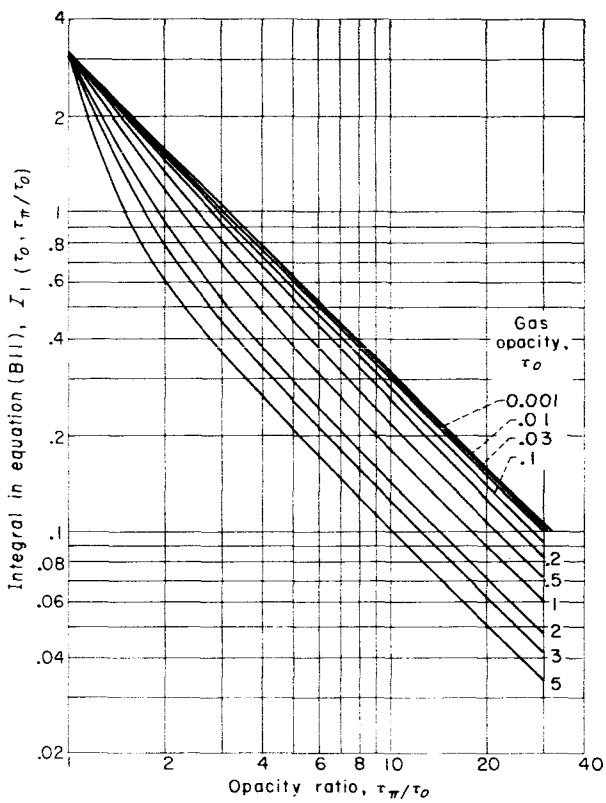

FIGURE 11.—Variation of integral in equation (B11) with opacity ratio.

$$I_1\left(\tau_o,\frac{\tau_\pi}{\tau_o}\right)=\int_{(\tau/\tau_o)=1}^{\tau_\pi/\tau_o}\frac{e^{-(\tau-\tau_o)}}{\left(\frac{\tau}{\tau_o}\right)^2}\beta\left(\frac{\tau}{\tau_o}\right)d\left(\frac{\tau}{\tau_o}\right);$$

$$\beta\left(\frac{\tau}{\tau_o}\right)=2\left(\frac{\tau}{\tau_o}\right)\Big/\sqrt{\left[\left(\frac{\tau}{\tau_o}\right)^2-1\right]\left[\left(\frac{\tau_\pi}{\tau_o}\right)^2-\left(\frac{\tau}{\tau_o}\right)^2\right]}.$$

CYLINDRICAL-SURFACE TO GAS EXCHANGE FACTORS

The problem now is to determine the radiative exchange between a ring (of infinitesimal width dx) on the interior cylindrical surface of the pipe and an infinitesimal volume dV at some point P in the gas. This situation is demonstrated in sketch (b).

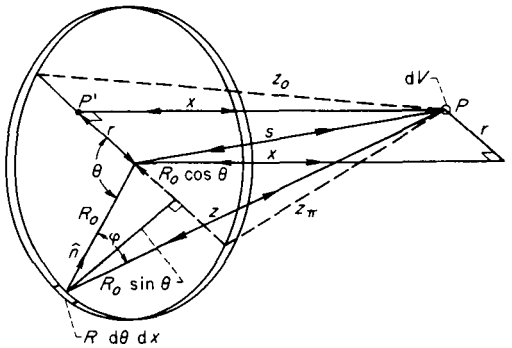

Sketch (b).

The radius of the surface ring on the pipe wall is R_o and the point P is at an axial distance x from the plane of the ring and at radius r from the centerline. The radiation emitted at unit emissive power from an infinitesimal arc of the ring that is transmitted to and absorbed at P is given by

$$dq_P=\frac{R_o\,d\theta\,dx}{\pi}\cos\varphi\,\frac{e^{-kz}}{z^2}\,k\,dV \qquad (B12)$$

where φ is the angle between the ray from the surface element $R_o\,d\theta\,dx$ to P and the normal to that surface element. The relation between z and θ is the same as before and is given by equation (B4). The law of cosines is used to find cos φ from the triangle $R_o zs$ formed by the infinitesimal surface element, the center of the surface ring, and point P. From the law of cosines

$$R_o^2+z^2-2R_o z\cos\varphi=s^2 \qquad (B13)$$

and from sketch (b), $s^2=r^2+x^2$; also z^2 may be found in terms of r, R_o, and x from equation (B4).

Combine these relations and solve for cos φ to obtain

$$\cos\varphi=\frac{R_o-r\cos\theta}{z} \qquad (B14)$$

Now, substitute equation (B14) in (B12) to eliminate cos φ; then equation (B12) may be integrated from 0 to 2π to obtain the contribution from the entire surface ring to the absorption at point P. When the result is reduced to terms of τ_o and τ_π, as before, the following equation is obtained:

$$\delta q_P=2k^4\,dV\,\frac{R_o^2}{\pi}\,dx\int_1^{\tau_\pi/\tau_o}\left(1-\frac{r}{R_o}\cos\theta\right)\frac{e^{-\tau}}{\tau^3}\,\beta\left(\frac{\tau}{\tau_o}\right)d\left(\frac{\tau}{\tau_o}\right) \qquad (B15)$$

where cos θ is a function of τ_π/τ_o and τ/τ_o and is given by equation (B8c). This situation is a little more complicated, since the resulting integral is now a function of three parameters, τ_o, τ_π, and the radius ratio r/R_o. Thus, the exchange factor $g_w(\vec{s}-\vec{P})$ between the ring surface $2\pi R_o\,dx$ and the volume dV is best given as the sum of two integrals, each of which is a function of only the two parameters τ_o and τ_π. Again, the parameterization is changed to $\left(\tau_o,\frac{\tau_\pi}{\tau_o}\right)$ for the same reasons given earlier. Thus, the result is

$$g_w(\vec{s}-\vec{P})=g_w\left(\tau_o,\frac{\tau_\pi}{\tau_o},\frac{r}{R_o}\right)$$
$$=\frac{k^3}{\pi^2}R_o\frac{e^{-\tau_o}}{\tau_o^3}\left[\int_1^{\tau_\pi/\tau_o}\frac{e^{-(\tau-\tau_o)}}{\left(\frac{\tau_o}{\tau}\right)^3}\beta\left(\frac{\tau}{\tau_o}\right)d\left(\frac{\tau}{\tau_o}\right)\right.$$
$$\left.-\frac{r}{R_o}\int_1^{\tau_\pi/\tau_o}\frac{e^{-(\tau-\tau_o)}}{\left(\frac{\tau_o}{\tau}\right)^3}(\cos\theta)\beta\left(\frac{\tau}{\tau_o}\right)d\left(\frac{\tau}{\tau_o}\right)\right] \qquad (B16)$$

The integrals

$$I_2\left(\tau_o,\frac{\tau_\pi}{\tau_o}\right)=\int_1^{\tau_\pi/\tau_o}\frac{e^{-(\tau-\tau_o)}}{\left(\frac{\tau}{\tau_o}\right)^3}\beta\left(\frac{\tau}{\tau_o}\right)d\left(\frac{\tau}{\tau_o}\right), \qquad (B17)$$

$$I_3\left(\tau_o,\frac{\tau_\pi}{\tau_o}\right)=\int_1^{\tau_\pi/\tau_o}\frac{e^{-(\tau-\tau_o)}}{\left(\frac{\tau}{\tau_o}\right)^3}(\cos\theta)\beta\left(\frac{\tau}{\tau_o}\right)d\left(\frac{\tau}{\tau_o}\right) \qquad (B18)$$

are plotted in figures 12 and 13, respectively.

END-SURFACE TO GAS EXCHANGE FACTORS

Here, it is desired to derive the relation for the radiative exchange between an annular ring surface element of radius R and width dR on one of the ends and an infinitesimal volume at some point P in the gas. Sketch (c) demon-

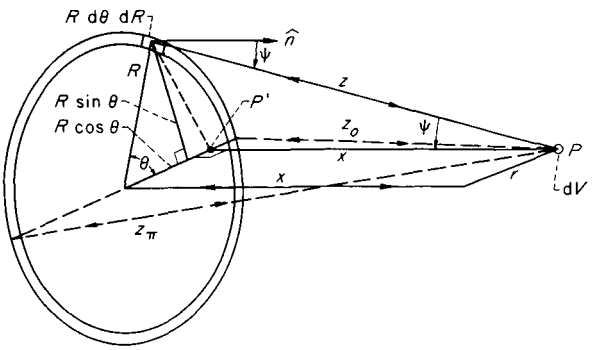

Sketch (c).

strates this situation, and the nomenclature is the same as that used for the previous sketches. The radiation emitted at unit emissive power from an infinitesimal arc of the annular ring that is transmitted to and absorbed at P is given by

$$dq_P=\frac{R\,d\theta\,dR}{\pi}\cos\psi\,\frac{e^{-kz}}{z^2}\,k\,dV \qquad \text{(B19)}$$

where ψ is the angle between the normal to the surface element and the ray from the element to point P. In this case, $\cos\psi$ is very simply given by

$$\cos\psi=\frac{x}{z}$$

Substitute this relation for $\cos\psi$ in equation (B19) and integrate from 0 to 2π to obtain the contribution from the entire annular ring to the absorption at P in terms of τ_o and τ_π:

$$\delta q_P=2k^4\,dV\,\frac{R\,dR}{\pi}\,x\int_1^{\tau_\pi/\tau_o}\frac{e^{-\tau}}{\tau^3}\,\beta\left(\frac{\tau}{\tau_o}\right)d\left(\frac{\tau}{\tau_o}\right) \qquad \text{(B20)}$$

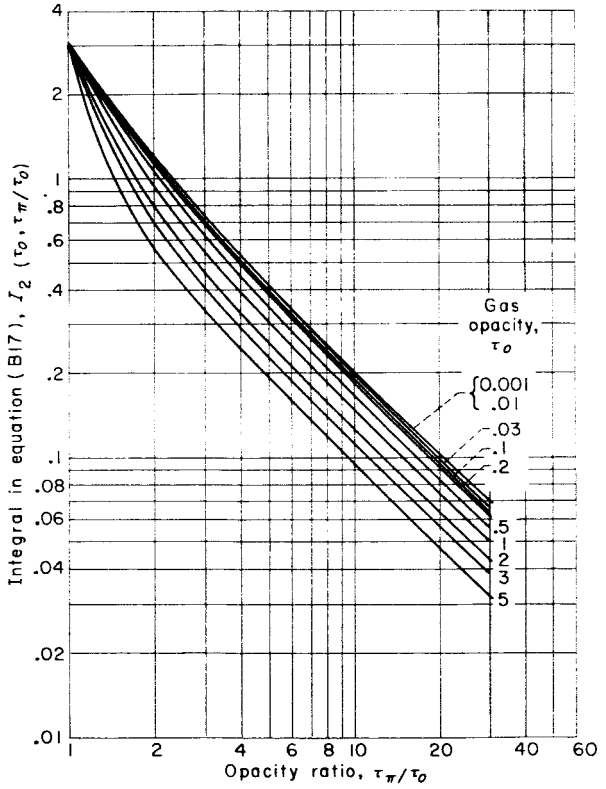

FIGURE 12.—Variation of integral in equation (B17) with opacity ratio.

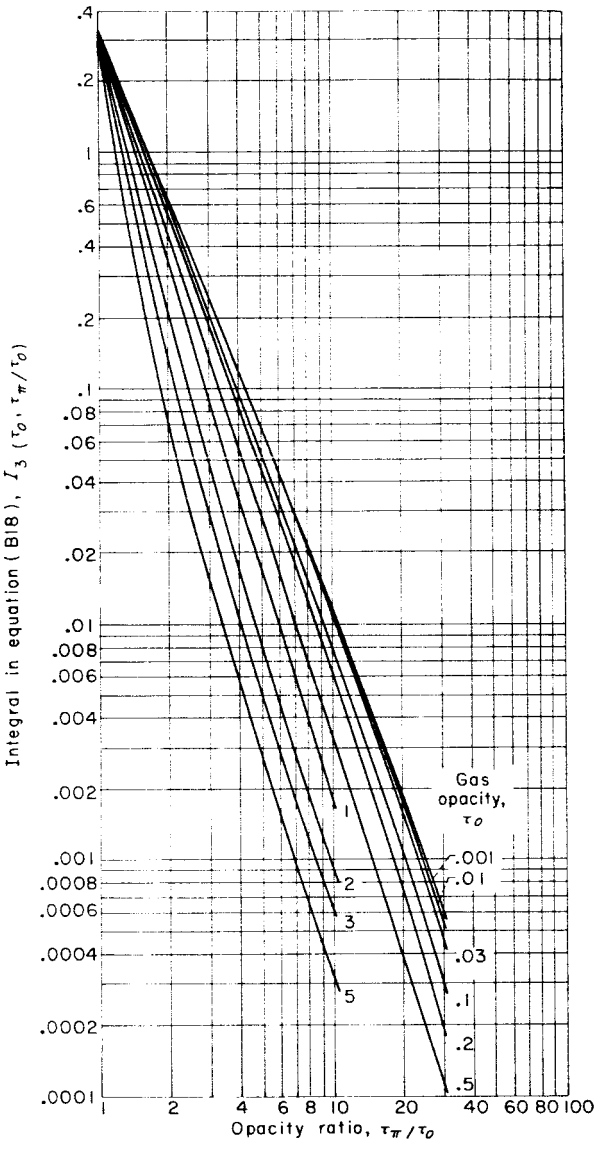

FIGURE 13.—Variation of integral in equation (B18) with opacity ratio.

$$I_2\left(\tau_o,\frac{\tau_\pi}{\tau_o}\right)=\int_{(\tau/\tau_o)=1}^{\tau_\pi/\tau_o}\frac{e^{-(\tau-\tau_o)}}{\left(\frac{\tau}{\tau_o}\right)^3}\,\beta\left(\frac{\tau}{\tau_o}\right)d\left(\frac{\tau}{\tau_o}\right);$$

$$\beta\left(\frac{\tau}{\tau_o}\right)=2\left(\frac{\tau}{\tau_o}\right)\Big/\sqrt{\left[\left(\frac{\tau}{\tau_o}\right)^2-1\right]\left[\left(\frac{\tau_\pi}{\tau_o}\right)^2-\left(\frac{\tau}{\tau_o}\right)^2\right]}.$$

$$I_3\left(\tau_o,\frac{\tau_\pi}{\tau_o}\right)=\int_{(\tau/\tau_o)=1}^{\tau_\pi/\tau_o}\frac{e^{-(\tau-\tau_o)}}{\left(\frac{\tau}{\tau_o}\right)^3}(\cos\theta)\beta\left(\frac{\tau}{\tau_o}\right)d\left(\frac{\tau}{\tau_o}\right);$$

$$\cos\theta=\left\{2\left(\frac{\tau}{\tau_o}\right)^2-\left[1+\left(\frac{\tau_\pi}{\tau_o}\right)^2\right]\right\}\Big/1-\left(\frac{\tau_\pi}{\tau_o}\right)^2;$$

$$\beta\left(\frac{\tau}{\tau_o}\right)=2\left(\frac{\tau}{\tau_o}\right)\Big/\sqrt{\left[\left(\frac{\tau}{\tau_o}\right)^2-1\right]\left[\left(\frac{\tau_\pi}{\tau_o}\right)^2-\left(\frac{\tau}{\tau_o}\right)^2\right]}.$$

Thus, the exchange factor between the annular ring surface on the end of area $2\pi R\ \mathrm{d}R$ and the volume $\mathrm{d}V$ at point P is given by

$$g_e(\vec{s}-\vec{P})=g_e\left(\tau_o,\frac{\tau_\pi}{\tau_o}\right)$$
$$=\frac{k^3}{\pi^2}x\frac{e^{-\tau_o}}{\tau_o^3}\int_1^{\tau_\pi/\tau_o}\frac{e^{-(\tau-\tau_o)}}{\left(\frac{\tau}{\tau_o}\right)^3}\beta\left(\frac{\tau}{\tau_o}\right)\mathrm{d}\left(\frac{\tau}{\tau_o}\right) \quad \text{(B21)}$$

The integral

$$I_2\left(\tau_o,\frac{\tau_\pi}{\tau_o}\right)=\int_1^{\tau_\pi/\tau_o}\frac{e^{-(\tau-\tau_o)}}{\left(\frac{\tau}{\tau_o}\right)^3}\beta\left(\frac{\tau}{\tau_o}\right)\mathrm{d}\left(\frac{\tau}{\tau_o}\right) \quad \text{(B17)}$$

was described earlier.

SURFACE TO SURFACE EXCHANGE FACTORS

There are three distinct surface to surface exchange factors: h_{ww}, the cylindrical-ring-surface to cylindrical-ring-surface exchange factor; $h_{we}=h_{ew}$, the cylindrical-ring-surface to end-annular-ring-surface exchange factor, and h_{ee}, the end-annular-ring-surface to end-annular-ring-surface exchange factor. Most of the basic relations that are needed in the derivations of these surface to surface exchange factors have already been discussed and will not be repeated. The graphics of the present situations are similar to those given in sketches (b) and (c).

Thus, for the case of h_{ww}, consider an infinitesimal area $\mathrm{d}A$ at a point Q on the cylindrical surface of the pipe wall that receives radiation from a ring surface of infinitesimal width $\mathrm{d}x$ on the pipe wall, and let x be the axial distance from Q to the plane of this ring. The point Q lies, of course, on the same radius as the ring. Thus, the radiation exchange at unit emissive power from an infinitesimal arc of the ring to $\mathrm{d}A$ at Q is given by

$$\mathrm{d}q_Q=\frac{R_o\,\mathrm{d}\theta\,\mathrm{d}x}{\pi}\mathrm{d}A\cos^2\varphi\frac{e^{-kz}}{z^2} \quad \text{(B22)}$$

Using the relation for $\cos\varphi$ from equation (B14), noting that here $r=R_o$, and integrating over the whole ring yield the following result in terms of τ_o and τ_π:

$$\delta q_Q=2\frac{R_o^3k^4\,\mathrm{d}x}{\pi}\mathrm{d}A\int_1^{\tau_\pi/\tau_o}$$
$$(1-\cos\theta)^2\frac{e^{-\tau}}{\tau^4}\beta\left(\frac{\tau}{\tau_o}\right)\mathrm{d}\left(\frac{\tau}{\tau_o}\right) \quad \text{(B23)}$$

Equation (B23) can then be integrated over the ring of which $\mathrm{d}A$ is a surface element to obtain the total exchange between the two surface rings. Thus, the exchange factor between two surface rings on the cylindrical wall, each of infinitesimal area $2\pi R_o\ \mathrm{d}x$ and separated by a distance x is

$$h_{ww}(\vec{s}-\vec{Q})=h_{ww}\left(\tau_o,\frac{\tau_\pi}{\tau_o}\right)$$
$$=\frac{R_o^2k^4}{\pi^2}\frac{e^{-\tau_o}}{\tau_o^4}\int_1^{\tau_\pi/\tau_o}(1-\cos\theta)^2$$
$$\frac{e^{-(\tau-\tau_o)}}{\left(\frac{\tau}{\tau_o}\right)^4}\beta\left(\frac{\tau}{\tau_o}\right)\mathrm{d}\left(\frac{\tau}{\tau_o}\right) \quad \text{(B24)}$$

The function

$$I_5\left(\tau_o,\frac{\tau_\pi}{\tau_o}\right)=\int_1^{\tau_\pi/\tau_o}\frac{e^{-(\tau-\tau_o)}}{\left(\frac{\tau}{\tau_o}\right)^4}(1-\cos\theta)^2\beta\left(\frac{\tau}{\tau_o}\right)\mathrm{d}\left(\frac{\tau}{\tau_o}\right) \quad \text{(B25)}$$

is plotted in figure 15. It is interesting to note that in this case $\tau_o=kx$ and $\tau_\pi/\tau_o=\sqrt{1+4R_o^2/x^2}$. Equation (B8c) is used to express $\cos\theta$ in equation (B25) as a function of τ/τ_o and τ_π/τ_o.

The exchange factor h_{we} is derived in an almost identical manner. Let the emitting surface ring be on the cylindrical wall as before, and let $\mathrm{d}A$ be at point Q on an end surface at radius r. Then the transmission at unit emissive power from an infinitesimal arc of the wall surface to Q is given by

$$\mathrm{d}q_Q=\frac{R_o\,\mathrm{d}\theta\,\mathrm{d}x}{\pi}\mathrm{d}A\cos\varphi\cos\psi\frac{e^{-kz}}{z^2} \quad \text{(B26)}$$

Using the relations for $\cos\varphi$ and $\cos\psi$ derived earlier and integrating over the ring as before yield

$$\delta q_Q=2\frac{R_o^2k^4\,\mathrm{d}x}{\pi}\mathrm{d}A$$
$$x\int_1^{\tau_\pi/\tau_o}\left(1-\frac{r}{R_o}\cos\theta\right)\frac{e^{-\tau}}{\tau^4}\beta\left(\frac{\tau}{\tau_o}\right)\mathrm{d}\left(\frac{\tau}{\tau_o}\right) \quad \text{(B27)}$$

Again, this expression may be integrated over $\mathrm{d}A$ to obtain the exchange between a ring on the cylindrical wall of area $2\pi R_o\ \mathrm{d}x$ and an annular ring on the end surface of area $2\pi r\ \mathrm{d}r$. Because of the dependence of the result on radius ratio r/R_o, it again makes sense to split the expression for exchange factor into two integrals, each of which is dependent on only $\left(\tau_o,\frac{\tau_\pi}{\tau_o}\right)$. Thus, the exchange

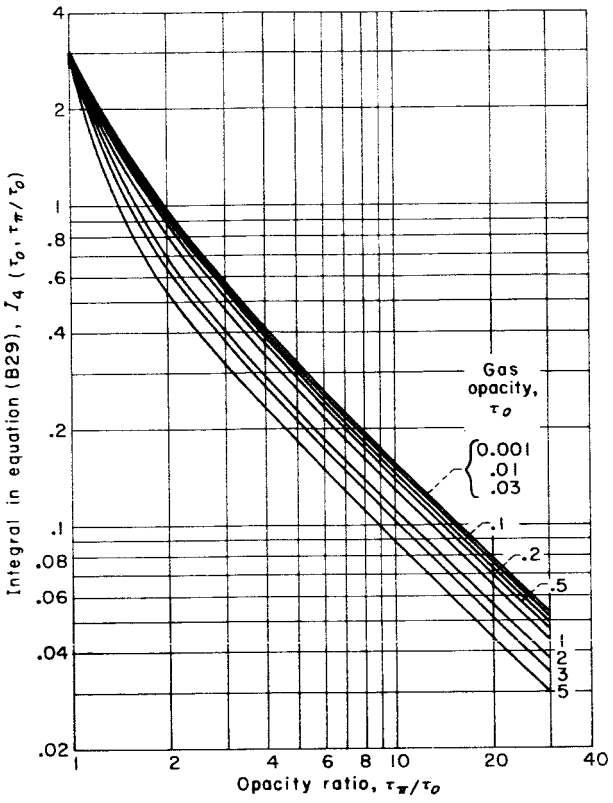

FIGURE 14.—Variation of integral in equation (B29) with opacity ratio.

$$I_4\left(\tau_o, \frac{\tau_\pi}{\tau_o}\right)=\int_{\tau/\tau_o=1}^{\tau_\pi/\tau_o} \frac{e^{-(\tau-\tau_o)}}{\left(\frac{\tau}{\tau_o}\right)^4}\beta\left(\frac{\tau}{\tau_o}\right)\mathrm{d}\left(\frac{\tau}{\tau_o}\right);$$

$$\beta\left(\frac{\tau}{\tau_o}\right)=2\left(\frac{\tau}{\tau_o}\right)\Big/\sqrt{\left[\left(\frac{\tau}{\tau_o}\right)^2-1\right]\left[\left(\frac{\tau_\pi}{\tau_o}\right)^2-\left(\frac{\tau}{\tau_o}\right)^2\right]}.$$

factor between the two infinitesimal areas given previously becomes

$$h_{we}(\vec{s}-\vec{Q})=h_{we}\left(\tau_o, \frac{\tau_\pi}{\tau_o}\right)$$
$$=\frac{R_o x}{\pi^2}k^4\frac{e^{-\tau_o}}{\tau_o^4}\left[\int_1^{\tau_\pi/\tau_o}\frac{e^{-(\tau-\tau_o)}}{\left(\frac{\tau}{\tau_o}\right)^4}\mathrm{d}\theta - \frac{r}{R_o}\int_{\tau_o}^{\tau_\pi}\frac{e^{-(\tau-\tau_o)}}{\left(\frac{\tau}{\tau_o}\right)^4}\cos\theta\,\mathrm{d}\theta\right] \quad \text{(B28)}$$

The functions

$$I_4\left(\tau_o, \frac{\tau_\pi}{\tau_o}\right)=\int_1^{\tau_\pi/\tau_o}\frac{e^{-(\tau-\tau_o)}}{\left(\frac{\tau}{\tau_o}\right)^4}\beta\left(\frac{\tau}{\tau_o}\right)\mathrm{d}\left(\frac{\tau}{\tau_o}\right) \quad \text{(B29)}$$

and

$$I_6\left(\tau_o, \frac{\tau_\pi}{\tau_o}\right)=\int_1^{\tau_\pi/\tau_o}\frac{e^{-(\tau-\tau_o)}}{\left(\frac{\tau}{\tau_o}\right)^4}(\cos\theta)\beta\left(\frac{\tau}{\tau_o}\right)\mathrm{d}\left(\frac{\tau}{\tau_o}\right) \quad \text{(B30)}$$

are plotted in figures 14 and 16, respectively.

Finally, in deriving h_{ee}, the exchange factor between annular rings at opposite ends of the pipe, the same procedure is again used. The radiation transferred per unit emissive power from an infinitesimal arc of an annular ring on one end of area $2\pi r\,dr$ to an area dA at point Q at radius r' on the other end is

$$\mathrm{d}q_Q=\frac{r\,dr\,d\theta}{\pi}\,dA\cos^2\psi\,\frac{e^{-kz}}{z^2} \quad \text{(B31)}$$

Integration over the annular ring yields

$$\delta q_P=\frac{2rk^4}{\pi}\,dr\,dA\,x^2\int_1^{\tau_\pi/\tau_o}\frac{e^{-\tau}}{\tau^4}\beta\left(\frac{\tau}{\tau_o}\right)\mathrm{d}\left(\frac{\tau}{\tau_o}\right) \quad \text{(B32)}$$

where x is the axial distance between the two surfaces, and is, in this case, merely the length of the cylinder. Then in the same manner as for the previous cases, the exchange factor between the two annular surface rings on each end of area $2\pi r\,dr$ and $2\pi r'\,dr'$, respectively, becomes

$$h_{ee}(\vec{s}-\vec{Q})=h_{ee}\left(\tau_o, \frac{\tau_\pi}{\tau_o}\right)=\frac{k^4}{\pi^2}x^2\frac{e^{-\tau_o}}{\tau_o^4}$$
$$\int_1^{\tau_\pi/\tau_o}\frac{e^{-(\tau-\tau_o)}}{\left(\frac{\tau}{\tau_o}\right)^4}\beta\left(\frac{\tau}{\tau_o}\right)\mathrm{d}\left(\frac{\tau}{\tau_o}\right) \quad \text{(B33)}$$

The integral

$$\int_1^{\tau_\pi/\tau_o}\frac{e^{-(\tau-\tau_o)}}{\left(\frac{\tau}{\tau_o}\right)^4}\beta\left(\frac{\tau}{\tau_o}\right)\mathrm{d}\left(\frac{\tau}{\tau_o}\right)$$

has been previously discussed as $I_4\left(\tau_o, \frac{\tau_\pi}{\tau_o}\right)$.

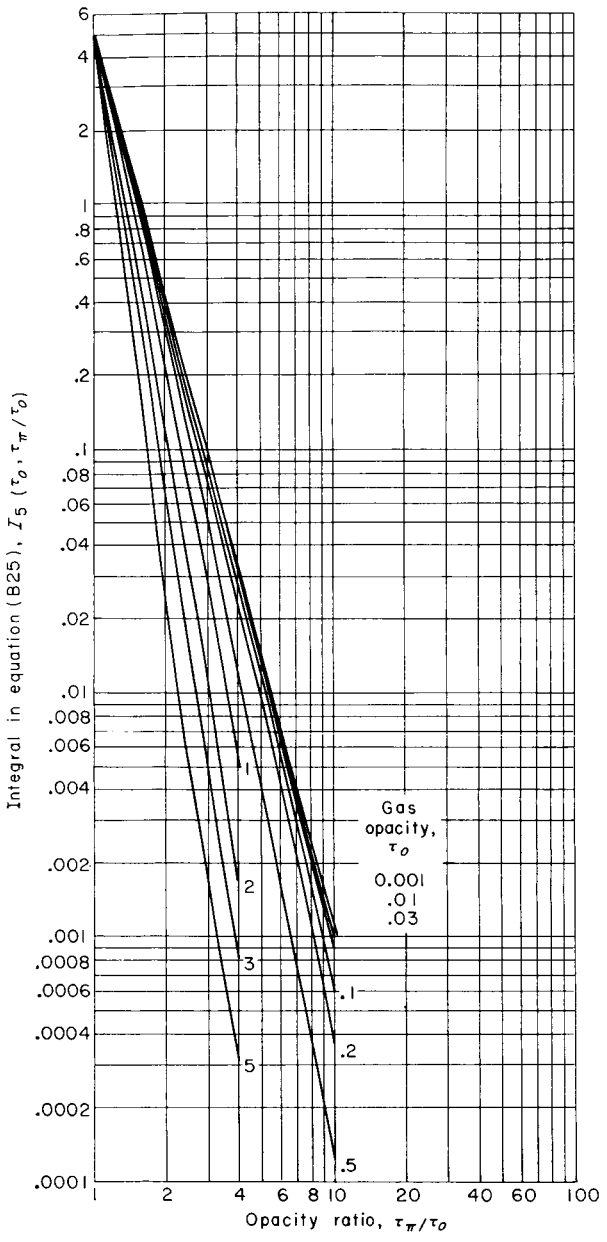

FIGURE 15.—Variation of integral in equation (B25) with opacity ratio.

$$I_5\left(\tau_o, \frac{\tau_\pi}{\tau_o}\right) = \int_{(\tau/\tau_o)=1}^{\tau_\pi/\tau_o} \frac{e^{-(\tau-\tau_o)}}{\left(\frac{\tau}{\tau_o}\right)^4} (1-\cos\theta)^2 \beta \left(\frac{\tau}{\tau_o}\right) \mathrm{d}\left(\frac{\tau}{\tau_o}\right);$$

$$(1-\cos\theta) = 2\left[\left(\frac{\tau}{\tau_o}\right)^2 - 1\right] \Big/ \left(\frac{\tau_\pi}{\tau_o}\right)^2 - 1;$$

$$\beta\left(\frac{\tau}{\tau_o}\right) = 2\left(\frac{\tau}{\tau_o}\right) \Big/ \sqrt{\left[\left(\frac{\tau}{\tau_o}\right)^2 - 1\right]\left[\left(\frac{\tau_\pi}{\tau_o}\right)^2 - \left(\frac{\tau}{\tau_o}\right)^2\right]}.$$

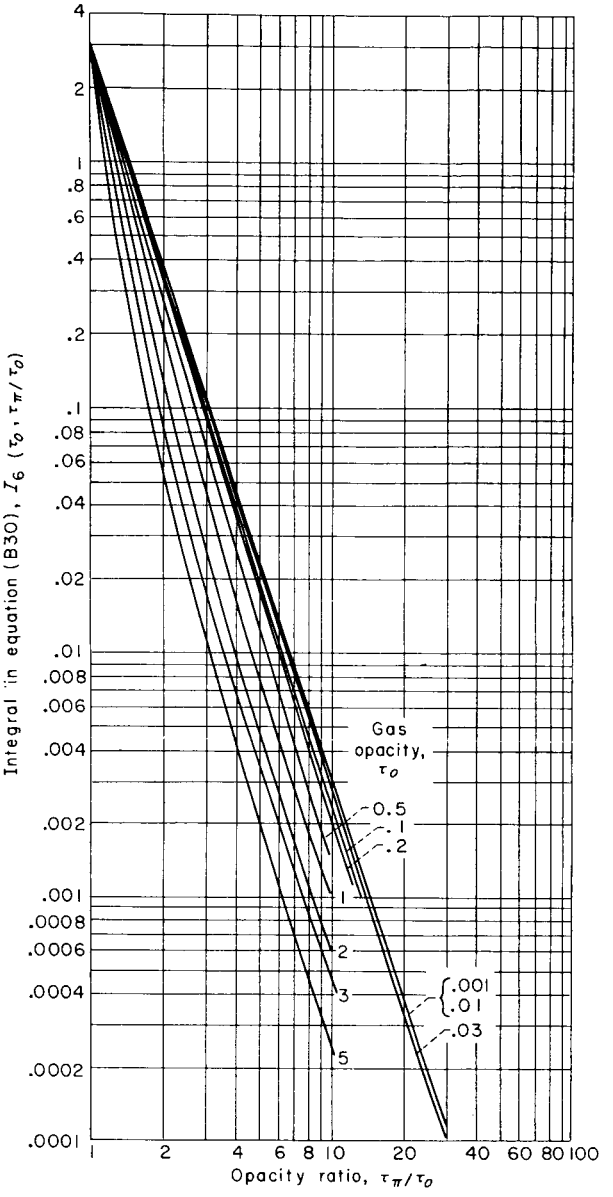

FIGURE 16.—Variation of integral in equation (B30) with opacity ratio.

$$I_6\left(\tau_o, \frac{\tau_\pi}{\tau_o}\right) = \int_{(\tau/\tau_o)=1}^{\tau_\pi/\tau_o} \frac{e^{-(\tau-\tau_o)}}{\left(\frac{\tau}{\tau_o}\right)^4} (\cos\theta)\beta \left(\frac{\tau}{\tau_o}\right) \mathrm{d}\left(\frac{\tau}{\tau_o}\right);$$

$$\cos\theta = \left\{2\left(\frac{\tau}{\tau_o}\right)^2 - \left[1+\left(\frac{\tau_\pi}{\tau_o}\right)^2\right]\right\} \Big/ 1 - \left(\frac{\tau_\pi}{\tau_o}\right)^2;$$

$$\beta\left(\frac{\tau}{\tau_o}\right) = 2\left(\frac{\tau}{\tau_o}\right) \Big/ \sqrt{\left[\left(\frac{\tau}{\tau_o}\right)^2 - 1\right]\left[\left(\frac{\tau_\pi}{\tau_o}\right)^2 - \left(\frac{\tau}{\tau_o}\right)^2\right]}.$$

APPENDIX C

COMPUTATION OF GAS-ZONE TO GAS EXCHANGE INTEGRALS

Consider the problem of computing the radiation transfer from one of the toroidal gas zones to an infinitesimal volume located at the center of the cross section of one of the other zones. A cross section of the cylindrical channel in which this situation is illustrated is shown in figure 17. The gas zones are toroidal rings of rectangular cross section, as shown, whose axis is the centerline of the cylinder. The interior of the cross section of the $(m, n)^{\text{th}}$ zone is described by the rectangular coordinate system (ξ, η) whose origin is at the center of the cross section, as shown in figure 17. The position vector of any point in the cross section of the $(m, n)^{\text{th}}$ gas zone is designated by $\vec{r}_{m,n}(\xi, \eta)$. The position vector of the infinitesimal volume at the center of the cross section of the $(i,j)^{\text{th}}$ zone that is being irradiated by the $(m,n)^{\text{th}}$ zone is $\vec{R}_{i,j}$. The region enclosing the $(m,n)^{\text{th}}$ zone and the point $\vec{R}_{i,j}$ consists of a uniformly absorbing gray medium. The $(m,n)^{\text{th}}$ zone may be thought of as being built up by a series of rings, each of which has an infinitesimal cross-sectional area $d\xi\ d\eta$. The emissive-power distribution in the zone is a linear function of (ξ, η) given by equation (3). The exchange factor between one of the gas-ring sources at position $\vec{r}_{m,n}(\xi, \eta)$ in the $(m, n)^{\text{th}}$ zone, and the infinitesimal volume dV at $\vec{R}_{i,j}$ is given by

$$F(\vec{s}) = 2\pi\rho f\left(\tau_o, \frac{\tau_\pi}{\tau_o}\right)$$

where ρ is the radius of the gas-ring source through $\vec{r}_{m,n}(\xi, \eta)$,

$$\vec{s} = \vec{r}_{m,n}(\xi, \eta) + \vec{R}_{i,j}$$

and

$$\tau_o = k|\vec{s}|$$

Since the nature of the exchange factors $f(\vec{s})$ derived in appendix B is such that the volume integrals over the gas zones become surface integrals over the zone cross sections, the radiation from the entire $(m,n)^{\text{th}}$ zone that is absorbed by dV at $\vec{R}_{i,j}$ is given by

$$\delta q = k\,dV_{i,j}\iint \sigma T^4(\xi, \eta) F[\vec{r}_{m,n}(\xi, \eta) - \vec{R}_{i,j}]\,d\xi\ d\eta \tag{C1}$$

Substitution of equation (3) for $T^4(\xi, \eta)$ in equation (C1) gives

$$\frac{\delta q}{k\,dV_{i,j}} = \sigma T^4_{m,n}\iint f(\vec{s})\,d\xi\ d\eta + \frac{\sigma(T^4_{m\pm1,n} - T^4_{m,n})}{\xi_o}\iint \xi F(\vec{s})\,d\xi\,d\eta + \frac{\sigma(T^4_{m,n\pm1} - T^4_{m,n})}{\eta_o}\iint \eta F(\vec{s})\,d\xi\ d\eta \tag{C2}$$

where $\sigma T^4_{m,n}$ is the emissive power at the center of the cross section of the $(m,n)^{\text{th}}$ zone and $T_{m\pm1,n}$ and $T_{m,n\pm1}$ are the temperatures at the center

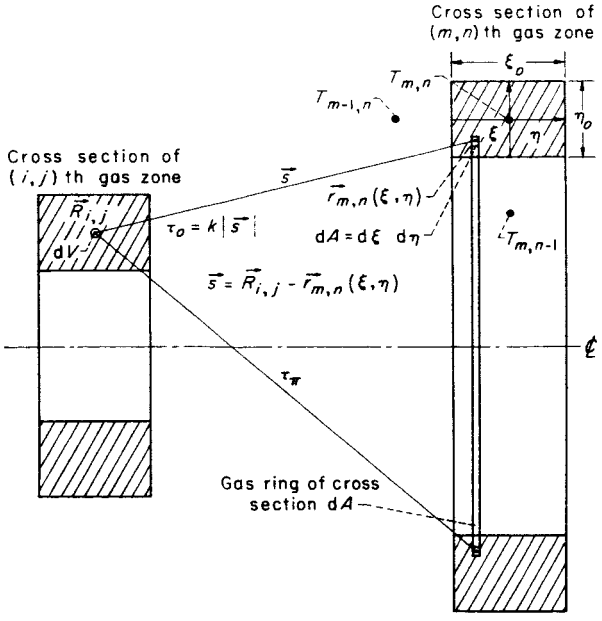

FIGURE 17.—Gas zone cross sections illustrating method of integrating exchange integral from $(m, n)^{\text{th}}$ gas-ring zone to dV at $\vec{R}_{i,j}$.

of the cross section of zones adjacent to the $(m, n)^{\text{th}}$ zones in the axial and radial directions, respectively, toward dV at position $\vec{R}_{i,j}$. As a result of these substitutions, the emissive powers do not enter into the integrations, and the integrals themselves that appear in equation (C2) are dependent only on the size of the $(m, n)^{\text{th}}$ zone and the relative axial and radial positions of dV at $\vec{R}_{i,j}$ with respect to the $(m, n)^{\text{th}}$ toroidal gas zone. The integration of the integrals that appear in equation (C2) is carried out numerically by dividing the zone cross section into a partition of small rectangles ($\Delta\xi$, $\Delta\eta$) and then summing the integrands over this partition. Thus, the triple volume integral that appears in equation (2) becomes a double integral over the surface of the zone cross section.

It is convenient to calculate the results in the following manner. Define

$$\bar{x}_{m,n}=\frac{\iint_{m,n}\xi F(\vec{s})\,d\xi\,d\eta}{\xi_o\iint_{m,n}F(\vec{s})\,d\xi\,d\eta} \qquad \text{where } -1/2<\bar{x}<1/2 \tag{C3}$$

and

$$\bar{r}_{m,n}=\frac{\iint_{m,n}\eta F(\vec{s})\,d\xi\,d\eta}{\eta_o\iint_{m,n}F(\vec{s})\,d\xi\,d\eta} \qquad \text{where } -1/2<\bar{r}<1/2 \tag{C4}$$

Again, $x_{m,n}$ and $\bar{r}_{m,n}$ are functions only of the size of the $(m, n)^{\text{th}}$ zone and the relative position of dV at $\vec{R}_{i,j}$ with respect to the $(m, n)^{\text{th}}$ zone. With the use of these definitions, the heat absorbed at dV due to emission from the $(m, n)^{\text{th}}$ zone is given by

$$\frac{\delta q}{k\,dV}=\sigma\left[(1-\bar{x}-\bar{r})T^4_{m,n}+\bar{x}T^4_{m\pm1,n}+\bar{r}T^4_{m,n\pm1}\right]\iint_{m,n}f(\vec{s})\,d\xi\,d\eta \tag{C5}$$

Equation (C5) is then used to evaluate the gas-zone to gas exchange integrals, which appear in equation (2), in terms of the gas-zone cross-sectional center temperatures.

REFERENCES

1. Einstein, Thomas H.: Radiant Heat Transfer to Absorbing Gases Between Parallel Flat Plates with Flow and Conduction. NASA TR R–154, 1963.
2. Adrianov, V. N., and Shorin, S. N.: Radiant Heat Transfer in a Flowing Radiating Medium. Izvestiia Akademii Nauk (SSSR), 1958. (AEC Trans. 3928.)
3. Hoffman, T. W., and Gauvin, W. H.: An Analysis of Spray Evaporation in a High-Temperature Environment. I. Radiant Heat Transfer to Clouds of Droplets and Particles. The Canadian Jour. Chem. Eng., vol. 39, no. 5, Oct. 1961, pp. 179–188.
4. Hottel, H. C., and Cohen, E. S.: Radiant Heat Exchange in a Gas-Filled Enclosure: Allowance for Nonuniformity of Gas Temperature. A.I.Ch.E. Jour., vol. 4, no. 1, Mar. 1958, pp. 3–14.
5. Sparrow, E. M., Usiskin, C. M., and Hubbard, H. A.: Radiation Heat Transfer in a Spherical Enclosure Containing a Participating, Heat-Generating Gas. Jour. Heat Transfer, ser. C, vol. 83, no. 2, May 1961, pp. 199–206.
6. Usiskin, C. M., and Sparrow, E. M.: Thermal Radiation Between Parallel Plates Separated by an Absorbing-Emitting Nonisothermal Gas. Int. Jour. Heat and Mass Transfer, vol. 1, no. 1, June 1960, pp. 28–36.
7. Deissler, R. G.: Diffusion Approximation for Thermal Radiation in Gases with Jump Boundary Condition. Paper 63–HT–13, ASME, 1963.

U.S. GOVERNMENT PRINTING OFFICE: 1963